PMComanchePekNPEm Resource

From: Monarque, Stephen
Sent: Thursday, March 04, 2010 1:30 PM
To: Seber, Dogan; Bauer, Laurel; Magee, Michael
Cc: ComanchePeakCOL Resource
Subject: FW: Seismic Sensitivity Study
Attachments: TXNB-10016 GSV-01 & -02.pdf

Importance: High

From: John.Conly@luminant.com [mailto:John.Conly@luminant.com]
Sent: Wednesday, March 03, 2010 5:52 PM
To: rjb@nei.org; david.beshear@txu.com; Biggins, James; rbird1@luminant.com; mike.blevins@luminant.com; Dennis.Buschbaum@luminant.com; russell_bywater@mnes-us.com; JCaldwell@luminant.com; Ronald.Carver@luminant.com; cp34update@certrec.com; Ciocco, Jeff; Timothy.Clouser@luminant.com; Collins, Elmo; John.Conly@luminant.com; Carolyn.Cosentino@luminant.com; brock.degeyter@energyfutureholdings.com; nancy.douglas@txu.com; Eric.Evans@luminant.com; Rafael.Flores@luminant.com; sfrantz@morganlewis.com; Goldin, Laura; Hamzehee, Hossein; kazuya_hayashi@mnes-us.com; masaya_hoshi@mnes-us.com; mutsumi_ishida@mnes-us.com; Johnson, Michael; Kallan, Paul; masahiko_kaneda@mnes-us.com; kak@nei.org; nicholas_kellenberger@mnes-us.com; Allan.Koenig@luminant.com; Kramer, John; mlucas3@luminant.com; Fred.Madden@luminant.com; Matthews, David; tmatthews@morganlewis.com; Monarque, Stephen; Ashley.Monts@luminant.com; Bill.Moore@luminant.com; masanori_onozuka@mnes-us.com; Palmrose, Donald; ck_paulson@mnes-us.com; Plisco, Loren; Robert.Reible@luminant.com; jrund@morganlewis.com; jeff.simmons@energyfutureholdings.com; Singal, Balwant; nan_sirirat@mnes-us.com; Takacs, Michael; joseph_tapia@mnes-us.com; Tindell, Brian; Bruce.Turner@luminant.com; Vrahoretis, Susan; Ward, William; Matthew.Weeks@luminant.com; Willingham, Michael; Donald.Woodlan@luminant.com; diane_yeager@mnes-us.com
Cc: James.Hill2@luminant.com
Subject: Seismic Sensitivity Study

Luminant has submitted to the NRC the attached Project Report, which documents a three-calculation sensitivity study to evaluate the effect of alternative assumptions on the site response at the top of Layer C. If there are any questions regarding the study, please contact me or contact Don Woodlan (254-897-6887, Donald.Woodlan@luminant.com).

Thanks,

John Conly

Luminant
COLA Project Manager
(254) 897-5256

Hearing Identifier: ComanchePeak_COL_NonPublic
Email Number: 1466

Mail Envelope Properties (9C2386A0C0BC584684916F7A0482B6CA0B98ECEB4B)

Subject: FW: Seismic Sensitivity Study
Sent Date: 3/4/2010 1:30:03 PM
Received Date: 3/4/2010 1:30:13 PM
From: Monarque, Stephen

Created By: Stephen.Monarque@nrc.gov

Recipients:
"ComanchePeakCOL Resource" <ComanchePeakCOL.Resource@nrc.gov>
Tracking Status: None
"Seber, Dogan" <Dogan.Seber@nrc.gov>
Tracking Status: None
"Bauer, Laurel" <Laurel.Bauer@nrc.gov>
Tracking Status: None
"Magee, Michael" <Michael.Magee@nrc.gov>
Tracking Status: None

Post Office: HQCLSTR02.nrc.gov

Files	**Size**	**Date & Time**
MESSAGE	2584	3/4/2010 1:30:13 PM
TXNB-10016 GSV-01 & -02.pdf	6934891	

Options
Priority: High
Return Notification: No
Reply Requested: No
Sensitivity: Normal
Expiration Date:
Recipients Received:

Luminant

Rafael Flores
Senior Vice President &
Chief Nuclear Officer
rafael.flores@luminant.com

Luminant Power
P O Box 1002
6322 North FM 56
Glen Rose, TX 76043

T 254.897.5590
F 254.897.6652
C 817.559.0403

CP-201000340
Log # TXNB-10016

Ref. # 10 CFR 52

March 3, 2010

U. S. Nuclear Regulatory Commission
Document Control Desk
Washington, DC 20555
ATTN: David B. Matthews, Director
Division of New Reactor Licensing

SUBJECT: COMANCHE PEAK NUCLEAR POWER PLANT, UNITS 3 AND 4
DOCKET NUMBERS 52-034 AND 52-035
SUPPLEMENTAL INFORMATION REGARDING GEOLOGY SAFETY SITE VISIT

Dear Sir:

Luminant Generation Company LLC (Luminant) submits herein information to supplement the discussions during the geology safety site visit in July 2009 and ensuing conference calls. Luminant has performed a sensitivity study to evaluate the effect of alternative assumptions on the site response at the top of Layer C. Because all Category 1 structures will be founded directly on Layer C or a leveling fill concrete, the top of Layer C was also defined as the Foundation Input Response Spectra depth (FIRS1) hence, GMRS/FIRS1. The first sensitivity calculation evaluates the effect of the correlation coefficient between the shear-wave velocities at different depths in the synthetic profiles used to characterize uncertainty in site properties. The second calculation evaluates the effect of soil nonlinearity in the shallow profile, while incorporating the effect of the soils above Layer C in the manner recommended by ISG-017. The third calculation evaluates the effect of interbedded shale layers within Layer C, beneath the proposed construction site. Appendix 3 has been added to the Project Report, "Dynamic Profile," TXUT-001-PR-007, Revision 4 (attached) to document the results of these three sensitivity calculations.

Should you have any questions regarding this report, please contact Don Woodlan (254-897-6887, Donald.Woodlan@luminant.com) or me.

There are no commitments in this letter. I state under penalty of perjury that the foregoing is true and correct.

Executed on March 3, 2010.

Sincerely,

Luminant Generating Company LLC

Donald R. Woodlan for

Rafael Flores

Attachment: Project Report, "Dynamic Profile," TXUT-001-PR-007, Revision 4

Electronic distribution w/o attachment:

mike.blevins@luminant.com
Rafael.Flores@luminant.com
mlucas3@luminant.com
jeff.simmons@energyfutureholdings.com
Bill.Moore@luminant.com
Brock.Degeyter@energyfutureholdings.com
rbird1@luminant.com
Matthew.Weeks@luminant.com
Allan.Koenig@luminant.com
Timothy.Clouser@luminant.com
Ronald.Carver@luminant.com
David.Volkening@luminant.com
Bruce.Turner@luminant.com
Eric.Evans@luminant.com
Robert.Reible@luminant.com
donald.woodlan@luminant.com
John.Conly@luminant.com
JCaldwell@luminant.com
David.Beshear@txu.com
Ashley.Monts@luminant.com
Fred.Madden@luminant.com
Dennis.Buschbaum@luminant.com
Carolyn.Cosentino@luminant.com

Luminant Records Management

masahiko_kaneda@mnes-us.com
masanori_onozuka@mnes-us.com
ck_paulson@mnes-us.com
joseph_tapia@mnes-us.com
russell_bywater@mnes-us.com
diane_yeager@mnes-us.com
kazuya_hayashi@mnes-us.com
mutsumi_ishida@mnes-us.com
nan_sirirat@mnes-us.com
masaya_hoshi@mnes-us.com
rjb@nei.org
kak@nei.org
michael.takacs@nrc.gov
cp34update@certrec.com
michael.johnson@nrc.gov
David.Matthews@nrc.gov
Balwant.Singal@nrc.gov
Hossein.Hamzehee@nrc.gov
Stephen.Monarque@nrc.gov
jeff.ciocco@nrc.gov
michael.willingham@nrc.gov
john.kramer@nrc.gov
Brian.Tindell@nrc.gov
Donald.Palmrose@nrc.gov
Elmo.Collins@nrc.gov
Loren.Plisco@nrc.com
Laura.Goldin@nrc.gov
James.Biggins@nrc.gov
Susan.Vrahoretis@nrc.gov
sfrantz@morganlewis.com
jrund@morganlewis.com
tmatthews@morganlewis.com

ENERCON SERVICES, INC.	PROJECT REPORT COVER SHEET	NO. TXUT-001-PR-007	
		REV.	4
		PAGE NO.	1 of 36

COMANCHE PEAK
PROJECT REPORT

DYNAMIC PROFILE

Independent Review Required: X Yes ___ No

Prepared by: Stephanie Briggs **Date:** __03-01-2010__

Reviewed by: Chris Fuller **Date:** __03-01-2010__

Approved by: Frank Syms Joe Mancinelli **Date:** __03-01-2010__

STATE OF TEXAS
Frank H. Syms
Geology
License # 10533
LICENSED
PROFESSIONAL GEOSCIENTIST

PROJECT REPORT REVISION STATUS

REVISION	DATE	DESCRIPTION
0	12-02-07	Initial issue
1	09-16-09	Added Appendix 2 in Response to RAI 02.05.04-14. Also made editorial changes throughout the document.
2	09-24-09	Incorporates non-substantive editorial changes. Rev. 1 included an Independent Review for technical content. Rev. 2 review pertains only to editorial changes.
3	02-16-10	Addition of Appendix 3 to document site response sensitivity analysis.
4	03-01-10	Editorial correction to Appendix 3.

PAGE REVISION STATUS

PAGE NO.	REVISION	PAGE NO.	REVISION
1–2	4		
3-36	3		

APPENDIX REVISION STATUS

APPENDIX NO.	PAGE NO.	REVISION NO.	APPENDIX NO.	PAGE NO.	REVISION NO.
1	1 – 2	2	3	4	4
2	1 – 7	2	3	5-24	3
3	1 – 3	3			

CONTENTS

TABLES

FIGURES

APPENDIX

1.0 PURPOSE AND OVERVIEW

This document describes the methodology and data used to develop the Dynamic Profile for Comanche Peak Nuclear Power Plant Units 3 & 4 (CPNPP 3 & 4). The dynamic profile is provided as input to the ground motion studies for determining the Ground Motion Response Spectra (GMRS) and Foundation Input Response Spectra (FIRS) and consists of shear- and pressure-wave velocities and associated dynamic properties for the defined profile.

The profile is defined as the interval extending from near surface to seismic basement (defined by the depth at which a shear wave velocity of 9200 ft/sec and greater is reached) and is divided into the shallow profile and the deep profile. The shallow profile extends from near surface to about 550-ft depth and is characterized from borings, geophysical logs including suspension velocities, and laboratory test results. The deep profile extends from about 550-ft depth to seismic basement and is characterized from regional geologic maps and well data including core and geophysical logs. The resulting Dynamic Profile is composed of representative velocities and material properties including index, strength, and damping percentages.

Appendix 2 describes a sensitivity analysis performed to test the non-linear behavior of the site-specific profile including the input data and results.

Appendix 3 presents sensitivity analyses performed to evaluate several parameters respective to the site response.

2.0 DEVELOPMENT OF SHALLOW AND DEEP STRATIGRAPHY

The shallow stratigraphy was developed from geotechnical borings and geophysical logs. The deep stratigraphy was developed from information in the published literature and data from regional oil and gas wells.

2.1 Shallow Stratigraphy

One hundred and forty-five geotechnical borings (excluding cluster, off-set, and monitoring well borings) were drilled as part of the subsurface exploration activities for CPNPP 3 & 4

(Figure 1). A detailed description of the data and methodology for developing the shallow stratigraphy is provided in calculation TXUT-001-FSAR-2.5-CALC-004, *Engineering Stratigraphy*. Velocity data for the shallow profile was acquired from 15 of the geotechnical borings (Figure 1). The velocity profile was developed through a correlation of velocity measurements with the engineering stratigraphy. A detailed discussion of the analysis is provided in the calculation TXUT-001-FSAR-2.5-CALC-003, *Shallow Velocity Profile Development Slope Method.*

Comparison of the geophysical data logs and the geotechnical boring logs provided the basis for developing the stratigraphic model at CPNPP 3 & 4. Suspension shear (V_s) and pressure (V_p) wave velocity, natural gamma radiation, and resistivity measurements, provided in GeoVision Report 6573-01 (GeoVision, 2007), were used to define stratigraphic units identified within the geotechnical boring logs. Ten major stratigraphic units were identified within the subsurface at CPNPP 3 & 4 between the ground surface and about 550 ft below ground surface (elevation 294 ft). As shown in Figure 2, these 10 units are divided among three geologic formations, in order of depth: the Glen Rose formation, Twin Mountains formation, and the Mineral Wells formation.

The Glen Rose formation is the uppermost formation encountered and outcrops at the surface of the site and within surrounding drainage cuts and exposures. The Glen Rose limestone was divided into engineering stratigraphic units A through E (E1 to E3). Based on the borings drilled for CPNPP 3 & 4, the Glen Rose formation has a thickness of 169 to 228 ft. This variable thickness is primarily due to topographic differences between borings. The upper portion of the Glen Rose (units A and B) is composed of alternating thin to massive beds of limestone and shale, with shale becoming more prevalent towards the basal portion of the section. The bottom portion (units C through E) is composed of a thick section of limestone that alternates between packstone and wackestone and has several thin shale interbeds, such as unit D (see Figure 2). Appendix 3 describes the results of an extensive review of the lithology of Layer C and development of alternative models to analyze the effects of the non-linear behavior of shale on the site response.

A lithologic transition from limestone to sandstone marks the boundary between the base of the Glen Rose and the top of the Twin Mountains formation. The sandstone at the top of unit F, which is composed of limestone, shale, and sandstone, marks the gradational contact between the two formations. The Twin Mountains formation is primarily composed of interbedded sandstone and shale, ranges from 217 to 242 ft in thickness, and encompasses most of unit F and all of units G through I. Units G and I are composed of sandstone, and unit H is primarily shale with sandstone interbeds. Only one borehole (B-1012) was drilled deep enough (550 ft) to encounter the basal conglomerate of the Twin Mountains, Unit I, and the Pennsylvanian Mineral Wells formation. The top of the Mineral Wells formation was encountered at an elevation of 455 ft in depth (389 ft in elevation). The Mineral Wells formation is noted in this boring as a massive shale with interbeds of sandstone and is consistent with regional lithologic descriptions.

2.1.1 Correlation of the CPNPP 3 & 4 and CPSES 1 & 2 Stratigraphy

Qualitatively, the stratigraphic units identified in the Comanche Peak Steam Electric System Units 1 & 2 (CPSES 1 & 2) FSAR are very similar to the stratigraphic units picked for the current COLA investigation for CPNPP 3 & 4. Figure 3 shows the relative location of CPSES 1 & 2 to CPNPP 3 & 4. Construction photographs from CPSES 1 & 2, shown on Figure 4, show distinct beds of limestone and shale within the vertical exposures. The exposures of the Glen Rose formation documented in these photographs exhibit flat-lying (no apparent dip) limestone and shale beds of various thicknesses. Descriptions provided within the CPSES 1 & 2 FSAR correspond with descriptions of engineering layers A, B1 and B2, and C from the CPNPP 3 & 4 site.

Velocity data provided in the Dames & Moore Cross-Hole Data Report, *Generalized Subsurface Profile and Seismic Wave Velocities,* was also used to compare the site stratigraphy between CPSES 1 & 2 and CPNPP 3 & 4. Figure 5 compares the engineering stratigraphy layers of CPSES 1 & 2 and CPNPP 3 & 4, plotted at their respective elevations. The elevations of each engineering layer in CPSES 1 & 2 were found to differ by an average of 10 ft, or horizons in the profile from CPSES 1 & 2 have elevations about 10 ft below the elevations of the same horizons beneath CPNPP 3 & 4. Regional dip of the area is roughly 25 ft per mile to the southeast (Sellards et al., 1932). Given that CPNPP 3 & 4 are approximately 2000 ft NW (or updip) of CPSES 1 & 2, the difference is explained by and is consistent with the regional dip of the units. This comparison was then used as a basis to compare the stratigraphy between the site locations as well as to compare velocity profiles developed from independent measurements and techniques.

2.2 Deep Stratigraphy

A variety of regional information was used to determine the deep stratigraphy for CPNPP 3 & 4. Stratigraphic and velocity data were acquired from published literature and regional oil and gas wells. Figure 6 shows the location of wells used to determine deep stratigraphic units (summarized in Table 1 and Table 2) and the two wells that provided velocity data. Figure 7 shows the interpreted stratigraphy and V_p logs for two regional wells used to develop the deep profile.

The resulting deep stratigraphic profile (summarized in Table 3) begins in the lower Pennsylvanian Strawn group, which contains the Mineral Wells formation, the deepest unit defined as part of the shallow profile in Section 2.1. The remainder of the Strawn Series is lithologically similar to the Mineral Wells and consists of shales and intebedded sandstones and limestones. Included within the Strawn Series are the Garner and Millsap Lake formations. Below the Strawn is the Atoka Group which includes the Atoka Sand, the Smithwick Shale, and the Big Saline Conglomerate. The top of the Atoka Group, the Atoka sand, is shale interbedded with sands and limestones. The sandstone layers have an average thickness of about 30 ft (Thompson, 1982). To the north and west of the study area, the upper portion of the Atoka Group includes the Caddo Reef, a massive limestone. In Sommervell County, however, located closer to the Ouachita thrust belt, deposition was more terrigenous (Thompson, 1982). Beneath the Atoka sand, the Smithwick is primarily a black shale, with a thickness that varies from 300 to 600 ft (Sellards et al., 1932). Below the Smithwick shale, the Big Saline Conglomerate has a variable thickness and pinches out just southeast of the site, so that at CPNPP 3 & 4 it has a projected thickness of only about 40 ft. Underlying the Atoka Group is the Marble Falls limestone. The upper portion of this unit is a dark-colored fossiliferous limestone (Sellards et al., 1932). The lower portion of the Marble Falls is interbedded dark limestone and gray-black shale, sometimes referred to as the Comyn Formation (Montgomery et al., 2005), and sometimes considered part of the Barnett Shale (Rathje & Olsen, 2007), which is stratigraphically below the Marble Falls. The Mississippian Barnett Shale (250 to 1000 ft thick, regionally) represents a gas source and reservoir in the region. The Barnett Shale unconformably overlies the top of the Ellenburger Group throughout most of the Fort Worth Basin, though in the northeastern portion of the basin the Upper Ordovician Viola and Simpson limestones intervene (Montgomery et al., 2005). The Cambrian to Ordovician Ellenburger limestone and a thin underlying clastic sequence rests unconformably on metamorphic basement in the Fort Worth Basin and was deposited in a passive continental margin setting (Montgomery et al., 2005).

The methods for determining stratigraphic elevations of units are listed in order of confidence and are noted in Table 2.

A. The top of the Strawn was measured in wells logged by WLA as the top of the Mineral Wells formation.

B. Using GEOMAP-stated elevations of horizons in the three nearest wells, the attitude of each horizon was determined and the elevation projected to the site location.

C. The CPNPP 3 & 4 site was projected onto the line of section of GEOMAPS cross section through two nearby wells (Squaw Creek and 1-Davis).

D. Horizon elevations determined from GEOMAPS structure contour maps.

For most stratigraphic units, more than one method was available for determining the elevation of a given horizon, and the standard deviation (σ_{top}) of the resulting elevations was used as an estimate of the error. Only a single elevation pick was determined for the top of the Big Saline and the top of the Atoka, thus, the average standard deviation in feet for the other stratigraphic units was applied as an estimate of the error for these units.

3.0 VELOCITY PROFILE DEVELOPMENT

Velocity data used to construct the Dynamic Profile consists of suspension shear (V_s) and pressure wave (V_p) velocities acquired from the 15 borings for the shallow profile; and principally pressure wave and limited shear wave data for the deep profile. The shallow velocity profile was constructed from the 15 suspension borings drilled for the CPNPP 3 & 4 investigation to depths of 150 to 550 ft (GeoVision Report 6573-01, Comanche Peak COL Geophysical Logging Rev 0). The deep velocity profile was constructed from velocity data acquired from wells located 2 to as much as 40 miles from the site (Figure 6). Velocity data for the regional deep profile was provided by the Texas Railroad Commission.

3.1 Shallow Velocity Profile

Development of the site velocity profile is detailed in TXUT-001-FSAR-2.5-CALC-003, *Shallow Velocity Profile Development Slope Method*. This calculation demonstrated the correlation between the engineering stratigraphy developed for the site, and the shear-wave and pressure-wave velocity field stratification. Changes in the wave travel time gradients were demonstrated to correspond with engineering layer boundaries defined by major changes in lithology (primarily limestone, shale, and sandstones). The vertical correspondence of velocity to lithology is also correlated from borehole to borehole throughout the site, demonstrating the continuity of layers across the area.

Layer velocities for every layer, in each boring, were calculated using the inverse of the slope of a line fit through the simulated down-hole travel times through each individual layer. The geometrical means of the representative layer velocity measurements were calculated to develop the shallow velocity profile (Figure 8). Representative layer velocity variations for the shallow velocity profile are provided by transformed standard deviations of the log deviants of each layer.

3.1.1 Comparison of Velocity Methods for the Shallow Profile

The velocities acquired from the 15 suspension log velocities were compared to velocities acquired by other methods at four of the borings, as well as velocities acquired from cross-hole methods at CPSES 1 & 2. Shear wave velocities were obtained by inversion of surface wave dispersion curves (SASW) at B-1000, B-1001, B-1012, and B-2000. Down-hole velocities were also obtained to a depth of about 140 ft in B-1000 and B-2000. This data set of SASW and down-hole provided an independent velocity comparison for about the upper 100 ft of the profile of the companion suspension borings. Cross-hole velocities obtained for CPSES 1 & 2 provided a comparison of independently acquired velocities for most of the shallow profile (about 525 ft depth).

Analysis of the suspension log data showed that engineering layer C exhibited very low variability from hole to hole in terms of its representative layer velocities. The layer C interface was consistently detected by all techniques and provides a standard to compare the velocity results from each method. The results from all velocity measurement methods are shown on Figure 10. This figure shows suspension log data for all 15 borings, the average profile velocities developed from the suspension logs, the geometric mean of the SASW shear wave results along with the geometric mean of the downhole V_s and V_p velocities for layer C and cross-hole data from CPSES 1 & 2.

The representative profile velocities for layer C were 5685 ft/sec for the shear-wave and 11324 ft /sec for the pressure-wave velocities. These velocities demonstrate low variability (5596–5803 V_s and 10952–11709 V_p at the two-sigma range for the log deviates) between borings. For comparison, the shear wave velocities for layer C from the four SASW inversions ranged from 5000–5250 ft /sec, which represents an approximately 10 percent lower result but which more closely approximates the cross-hole shear wave velocities for this layer. The down-hole data suffered from a low signal-to-noise ratio in the shallow portion of section. However, the down-hole shear wave velocity for layer C in B-1000 was 5456 ft/sec, which closely matches the integrated profile velocity for this layer obtained from the suspension log data. In contrast, the down-hole shear wave velocity obtained from B-2000, 4415 ft /sec, is significantly lower than the other techniques and is probably in error because of the poor data quality. Comparison of the cross-hole and suspension log data throughout the rest of the section indicates that they are in general agreement but show local variations on the order as those discussed above. The largest discrepancy appears to be layer E2, which shows lower shear- and pressure-wave results. Similar variations on the order of about 10% are seen in the pressure-wave inter-method comparison.

The shallow profile velocities compare well with both the SASW and down-hole velocities acquired within companion suspension log borings as well as with the velocities acquired from the cross-hole survey completed for CPSES 1 & 2. The correlation of velocity gradient with the engineering stratigraphy and the lateral continuity of the engineering units suggests that the suspension log data provides reproducible measurements for the shallow profile. Thus, velocities acquired from the 15 suspension log borings have been used to define the shallow velocity profile (Figure 8) as provided in Table 4.

3.2 Development of Regional Deep Velocity Profile

Velocity data for the deep profile was obtained from the Bureau of Economic Geology, the University of Texas-Austin, and the Texas Railroad Commission. Velocity data used to develop the deep velocity profile (Figure 10) came from the two nearest wells with available data (Figure 6)—the Quicksilver 1-Officers Club well (located 7 miles to the ENE in Hood County) and the Sun 1-Hallmark well (located about 40 miles to the west in Erath County). The Officers Club well provided V_p and V_s data from an elevation of -4900 to -8900 ft including the Smithwick Shale, the Big Saline Conglomerate, the Marble Falls Limestone, the Barnett Shale and the Ellenburger Limestone. The Sun Hallmark-1 well provided V_p data from an elevation of 1100 ft to -2500 ft including the Strawn Series, the Atoka Sand, the Smithwick Shale, the Big Saline Conglomerates, the Marble Falls and the Barnett Shale. In addition, boring B-1012 from the geotechnical study at the site penetrated the Mineral Wells formation of the Strawn Series and provided V_p and V_s data which was applied to the entire Strawn Series, given that lithology is homogenous throughout (see stratigraphic discussion in Section 2.2).

Harmonic mean velocities were calculated for each stratigraphic unit using the relation $V = \Sigma d_i / \Sigma (d_i/v_i)$; where d is the distance between two measured velocity, v, data points. Harmonic mean V_s and V_p values (Table 3) for the Strawn came from the Mineral Wells formation data from boring B-1012, the V_s and V_p values for the Smithwick Shale, the Big Saline

Conglomerate, the Marble Falls Limestone, the Barnett Shale and the Ellenburger Limestone were calculated from the Quicksilver 1-Officers Club well data, and the V_p value for the Atoka Sand was calculated from the Sun 1-Hallmark well data. The Atoka Sand is the only unit which did not have V_s data, and so a V_s value was estimated using a linear regression of the V_p and V_s data from the other units in Officers Club well (Appendix 1). In cases where there was more than one velocity log available for a given unit, the resulting harmonic velocities differed by generally less than 10%. For example, the Mineral Wells formation (part of the Strawn Series) logged at boring B-1012 has a harmonic velocity of 10485 ft/sec and the Strawn Series logged in the Sun Hallmark well has a harmonic velocity of 11188 ft/sec, a difference of about 6%.

For the velocity data error analysis, standard deviations from the harmonic mean of V_p and V_s within each stratigraphic unit were determined. The V_s standard deviation for the Atoka unit (which did not have V_s measurements) was calculated by applying the same proportion from the V_p standard deviation to the harmonic mean V_s value (e.g., $\sigma_{Vs} = V_s * (\sigma V_p / V_p)$).

3.2.1 Depth of Seismic Basement

At an elevation of about -3973 ft, the Marble Falls limestone records a V_s of about 10520 ft/sec. Though this unit is sufficiently fast to be considered seismic basement ($V_s > 9200$ ft/sec, shown with a grey bar in Figure 9), it is underlain by the seismically slow Barnett Shale. The top of the underlying Ellenburger limestone is mapped at an elevation of about -4443 ± 73 ft, which has a V_s of about 10906 ft/sec and is the best estimate for the top of seismic basement beneath CPNPP. This unit is sufficiently thick regionally, and the nearby Officers Club well indicates greater than 3000 ft of material with shear wave velocities greater than 9200 ft/sec. Thus, basement is defined as the top of the Ellenburger formation for CPNPP 3 & 4.

4.0 DYNAMIC PROFILE DEVELOPMENT

The shallow and deep stratigraphy were combined to develop a layered model representative of the CPNPP site extending to seismic basement. Both aleatory and epistemic uncertainties were evaluated and formed the basis for assigning variability on both stratigraphic control as well as the dynamic properties developed for each layer.

4.1 Profile Construction

The shallow and deep profiles, as described above, were combined by coupling the Strawn Group using the Mineral Wells formation, which is the deepest stratigraphic unit logged at CPNPP 3 & 4, and the shallowest unit characterized for the deep profile. Table 4 provides a summary of the Dynamic Profile including stratigraphic top elevations and associated velocities, as discussed in Sections 2.0 and 3.0, and material properties, as described in the following sections. Dynamic profiles for developing the Ground Motion Response Spectra (GMRS) and Foundation Input Response Spectra (FIRS) are described in TXUT-001-PR-011, *Foundation Interface Report*.

4.2 Stratigraphic Variance and Uncertainty

Site stratigraphy including the shallow and deep layering, shear and compression wave velocities, and dynamic properties are provided in Table 4. The uncertainties associated with the stratigraphy and velocities for the shallow profile are much less than those for the deep profile. Therefore, the range about the mean for the velocities reported in Table 3 has been treated differently.

The shallow profile has been extensively characterized from over 150 geotechnical borings and geologic mapping of the area. The profile has been stratified based on vertical changes in lithology that can be mapped laterally from boring to boring. Standard deviations for the top of each shallow profile layer are less than 2 ft for the upper 200 ft of the profile. The standard deviation for the layers defining the shallow profile from about 200 ft to about 500 ft range from about 1 to 5 ft. Velocity data for the shallow profile acquired from 15 suspension borings demonstrated a strong correlation between the layering and where simulated down-hole travel time gradient “breaks” occurred. The velocity measurements from the suspension log were also compared with down-hole, SASW and cross-hole measurements and were determined to provide the most repeatable measurements. This comparison between various methods was also used to develop the assigned variability as provided in Table 4. Details for development of the layering and corresponding velocities are provided in TXUT-001-FSAR-2.5-CALC-003, *Shallow Velocity Profile Development Slope Method,* and TXUT-001-FSAR-2.5-CALC-004, *Engineering Stratigraphy.*

The deep profile was developed from regional wells and results in a higher uncertainity in both the layering (stratigraphy) and velocity measurements as described above. Shear wave velocity measurements were available from a single well located about 6 miles from the site and was limited to about 4000 ft of data (from about 5000 ft depth to about 9000 ft depth). This data was used to develop a linear extrapolation to estimate shear wave velocity from available pressure wave velocities from other wells to complete the deep profile. Thus the epistemic uncertainty for the deep profile is much greater than the shallow profile.

The deep profile lacks a statistical basis for estimating a robust standard deviation for all layer velocities. The Coefficient of Variation (COV=standard deviation/mean) calculated as 31 percent for the Atoka formation demonstrated the highest COV for all deep profile layers. This is due, in part, to the bimodal distribution of rock types and corresponding velocities within this interbedded sand and shale unit. Nonetheless, the variability was conservatively estimated at 31 percent for all deep profile layers. The velocity range for the shallow profile was defined as 25 percent of the mean velocity of each layer. This range envelopes the suspension log R1-R2 velocities as well as the cross-hole, down-hole and SASW velocities providing a conservative means to capture both epistemic and aleatory uncertainty.

4.3 Calculation of Poisson's Ratio

Poisson's ratio (μ) for each stratigraphic layer was calculated from the representative shear (V_s) and pressure (V_p) wave velocity:

$$\mu = \frac{0.5\left(\frac{Vp}{Vs}\right)^2 - 1}{\left(\frac{Vp}{Vs}\right)^2 - 1}$$

For the shallow profile, the Poisson's ratio was derived from the representative velocities calculated for each respective engineering layer (see TXUt-001-FSAR-2.5-CALC-003).

Poisson's ratio for the deep profile utilized representative velocities for each of the regional stratigraphic units as described above in Section 3.2. The calculated Poisson's ratio values for each layer were compared to the general rock lithology as described above and are considered to be reasonable estimates.

4.4 Measurement of Unit Weights

Mean total (wet) unit weight values for each engineering layer for the shallow profile (Layer A to Strawn (MW)) was determined from laboratory testing. The number of tests by layer and the range of values is provided in Table 5.

No samples were available for the deep portions of the profile, thus unit weight values were estimated based on principal lithology of each unit and reasonable values were estimated based on engineering judgment. A value of 150 lbs/ft^3 was determined as a reasonable estimate to represent the deep profile.

4.5 Determination of Dynamic Properties

All critical structures are to be founded directly on the limestone (Layer C) or fill concrete. The shallow velocity profile, as described in Section 3.1, demonstrates that the site is underlain by soft to firm rock with velocities ranging from greater than 6000 ft/sec for limestone to 3000 ft/sec and greater for sandstones and shale within the depth interval of about 550 ft below the site. Below 550-ft depth, the shear wave velocity profile, estimated from compression wave velocities obtained from regional wells, is greater than about 7500 ft/sec. The stiffness of these units is expected to behave linearly for low- to high-strain levels. However, to evaluate the site response respective to non-linear properties, the Ground Motion Response Spectra (GMRS) was tested using both linear and non-linear properties assigned for each of the layers described below. Results of this analysis will provide the basis for performing the remaining site response.

4.5.1 Shear Modulus (G) and Damping

Low-strain shear modulus (G) for the shallow profile was calculated from shear wave velocities acquired from the 15 suspension logs (*Shallow Velocity Profile Development*, TXUT-001-FSAR-2.5-CALC-003), applying unit weight values as described in Section 4.3. The deep profile (below 400 ft) was calculated from the estimated shear wave velocities and a unit weight of 150 lbs/ft^3 for all deep layers. Material damping was estimated for each layer of the profile based on the principal lithology. To test the profile for sensitivity to non-linear behavior, a set of degradation curves based on lithology and depth were developed in consultation with Dr. Ken Stokoe. A sensitivity run using these non-linear properties is presented in Appendix 2. For the shallow profile, limestones, shales and sandstones were assigned damping ratios of 1.8, 3.2, and 2.5 respectively. For the deep profile, limestones, shales and sandstones were assigned damping ratios of 0.8, 1.0, and 1.0 respectively. See Table 4 for lower and upper bound values estimated for shear modulus (G) *and* G_{max} *and estimated* damping percentages.

The fill concrete shear modulus has been calculated from an assumed mean shear wave velocity (see Appendix 1) and unit weight. The damping percentage of 1.0% is based on judgment and is reasonable for concrete.

The compacted fill has been stratified into three layers characterized by assumed differences in shear-wave velocity, as shown in Table 4. Shear modulus has been calculated from an assumed mean shear-wave velocity for each of the three layers and the assumed unit weight. Low-strain damping percentages were assigned as 1.5 for the upper two layers with the lowermost layer assigned 1.0. Degradation curves for the compacted fill are provided for shear modulus and damping with each appropriate curve listed in Table 4.

5.0 REFERENCES

Dames & Moore, 1986, Report: Cross-Hole Geophysical Survey, Comanche Peak Steam Electric Station, Glen Rose, Texas, Volume 1.

TXUT-001-FSAR-2.5-CALC-003, *Shallow Velocity Profile Development Slope Method*, Rev. 0.

TXUT-001-FSAR-2.5-CALC-004, *Engineering Stratigraphy*, Rev. 0.

GEOMAPS Company, 2007, Structure contour maps from Barnett Shale, Central Texas and Fort Worth Basin Series.

GeoVision, 2007, Comanche Peak COL Geophysical Logging (Revision A), Report 6573-01 Rev. A.

Montgomery, S. L., Jarvie, D. M., Bowker, K. A., and Pollastro, R. M., 2005, Mississipian Barnett Shale, Fort Worth Basin, north-central Texas: Gas-shale play with multi-trillion cubic foot potential: *AAPG Bulletin*, v. 89, p. 155–175.

Rathje, E. M., Olson, J. E., 2007, Technical issues related to hydraulic fracturing and fluid extraction/injection near the Comanche Peak Nuclear Facility in Texas: unpublished white paper, personal communication, September 2007.

Sellards, E. H., Adkins, W. S., and Plummer, F. B., 1932, The Geology of Texas, Volume 1, Stratigraphy; The University of Texas Bulletin, No. 3232, Austin, TX.

Thompson, D. M., 1982, Atoka Group (Lower to Middle Pennsylvanian), Northern Fort Worth Basin, Texas: Terrigenous Depositional Systems, Diagenesis, and Reservoir Distribution and Quality; Bureau of Economic Geology Report of Investigations No. 125.

6.0 APPENDIX

Appendix 1. Calculation of V_s for Atoka Unit

Appendix 2 Non-linear Sensitivity Study

Appendix 3 Site Response Sensitivity Analysis

Table 1. Stratigraphic picks used in estimating deep stratigraphy beneath Comanche Peak Facility.

Operator	Taylor	Dallas	Mid-Continent	Kadane	Quicksilver	Davis	Dorchester	Sun	Davis	Mid-Continent
Lease	2-B Cravens	1-Hubbard	Squaw Creek	1-Bunl	Officers Club‡	1-Cousins	1-Davis	1-Hallmark‡	1-Cousins†	Squaw Creek†
Distance from site (miles)	2.4	2.7	4.6	5.1	6.1	6.6	6.7	39.8	6.6	4.6
Unit										
Strawn									90	500
Atoka		-1541	-1564	-1755		-1796		0	-110	-1560
Smithwick			-3614			-3836	-3368	-1000	-3910	-3630
Big Saline	-3743	-3896			-4240			-1779	-4040	-3860
Marble	-3831	-4006	-3856	-4155	-4405	-3979	-3583	-2105	-4040	-3970
Barnett		-4491	-4304	-4585	-4605	-4416	-3973	-2265	-4480	-4320
Ellenburger		-4691	-4514	-4825	-5070	-4633	-4223	-2409	-4690	-4520

‡ Well with velocity data

† Measured off GEOMAPS cross section

Table 2. Calculated stratigraphic picks for CPNPP 3 & 4 and standard deviation.

	Method				
	A	B	C	D	σ
Strawn	388		336		26
Atoka		-1814	-980		417
Smithwick		-3809	-3742		34
Big Saline			-3932		
Marble		-3973	-3998	-4060	37
Barnett		-4196	-4384	-4550	145
Ellenburger		-4443	-4588		73

A. Drilled with WLA wells.
B. Projection of GEOMAPS-stated stratigraphic picks in three nearest wells.
C. Projection of stratigraphic picks measured off GEOMAPS cross section.
D. Read off GEOMAPS structure contour maps.
Standard deviation (σ) calculated for each horizon using multiple picks from different methods.

Table 3. Best estimate of deep stratigraphy and velocities

Unit	Lithology	Elevation (ft)	σ_{top}	Thickness(ft)	V_p (ft/sec)	σ_{Vp}	V_s (ft/sec)	σ_{Vs}	Poissons Ratio
Strawn	Shales with few sands and limestones beds	388.1	26	2202	10627	1042	5546	784	0.32
Atoka	Sands and shales interbedded	-1814	63†	1995	13921	4278	7642	2375*	0.28
Smithwick	Shale	-3809	33	123	10894	1108	5557	533	0.32
Big Saline	Conglomerate	-3932	63†	41	18004	1973	10247	813	0.26
Marble Falls	Limestone	-3973	37	223	19740	999	10520	481	0.30
Barnett	Shale	-4196	145	247	12858	1697	7783	997	0.21
Ellenburger	Limestone	-4443	73	>3000	20382	997	10906	896	0.30

Notes

†Reported standard deviation in elevation (σ_{top}) is average of other units' standard deviations.
Strawn unit V_p & V_s values are from Mineral Wells formation logged at CPNPP Units 3 & 4 Boring 1012. Compare V_p value to Sun Hallmark Well harmonic mean of 11188.
Atoka unit V_s values are calculated from regression of other units' V_p and Vs data.
Smithwick unit V_p value reported from Officers Club well. Compare value to V_p harmonic mean from Sun Hallmark well of 11849.
Standard deviation (σ) in V_s estimated from the standard deviation in V_p.
* Standard deviation (σ) in V_s estimated from the standard deviation in V_p.

Table 4. Dynamic properties of subsurface rock materials. Sheet 1 of 4: Lithology and stratigraphy

Profile	Unit	Lithology	Depth from YG[3]	Mean Elv Top (MSL, ft)	Mean Elv σ, Top (ft)	Mean Thickness (ft)
	Fill Concrete	To be placed as needed from top of layer C	N/A	N/A	N/A	-
	Compacted Fill	Fill for excavation	0.0	822.0	N/A	3.0
			3.0	819.0	N/A	17.0
			20.0	802.0	N/A	20.0
	Fill/Residuum	Fill/Residuum/weathered limestone	-	847.0	N/A	-
Shallow Site Profile[1]	A	Limestone (will be removed)	-	834.0	12.1	36.0
	B1	Shale (will be removed)	24.0	798.0	1.8	8.0
	B2	Shale with limestone (will be removed)	32.0	790.0	1.8	8.0
	C	**Limestone (foundation layer)**	**40.0**	**782.0**	**1.8**	**65.0**
	D	Shale	105.0	717.0	1.5	3.0
	E1	Limestone	108.0	714.0	1.6	24.0
	E2	Limestone	132.0	690.0	1.0	34.0
	E3	Limestone	166.0	656.0	1.0	34.0
	F	Limestone with interbedded shales and sand	200.0	622.0	2.2	29.0
	G	Sandstone	229.0	593.0	4.0	80.0
	H	Shale	309.0	513.0	5.2	62.0
	I	Sandstone	371.0	451.0	3.3	63.0
	Strawn (MW)	Shales with sandstone and limestone beds	434.0	388.1	26.0	2202.0
Deep Site Profile[2]	Atoka[12]	Sands and shales interbedded	2636.0	-1814.0	417.0	1995.0
	Smithwick	Shale	4631.0	-3809.0	34.0	123.0
	Big Saline[12]	Conglomerate and sandstones	4754.0	-3932.0	122.0	41.0
	Marble Falls	Limestone	4795.0	-3973.0	37.0	223.0
	Barnett	Shale	5018.0	-4196.0	145.0	247.0
	Ellenburger	Limestone	5265.0	-4443.0	73.0	>3000

Table 4. Dynamic properties of subsurface rock materials. Sheet 2 of 4: shear- (V_s) and pressure-wave (V_p) velocity and Poisson's ratio (cont.).

		Depth from YG[3]	Mean Vs	+Variability[4]	-Variability[4]	Mean Vp	+Variability[4]	-Variability[4]	Poisson's Ratio[8]
		(ft)	(ft/sec)	(ft/sec)	(ft/sec)	(ft/sec)	(ft/sec)	(ft/sec)	
	Fill Concrete	N/A	6800.0	7300.0	6300.0	-	-	-	0.20
	Compacted Fill	0.0	650.0	975.0	325.0	-	-	-	0.35
		3.0	800.0	1200.0	400.0	-	-	-	0.35
		20.0	1000.0	1500.0	500.0	-	-	-	0.35
	Fill/Residuum	-	-	-	-	-	-	-	-
Shallow Site Profile[1]	A	-	3548.0	4435.0	2661.0	8788.0	10985.0	6591.0	0.40
	B1	24.0	2609.0	3261.3	1956.8	6736.0	8420.0	5052.0	0.41
	B2	32.0	2716.0	3395.0	2037.0	7640.0	9550.0	5730.0	0.43
	C	**40.0**	**5685.0**	7106.3	4263.8	**11324.0**	14155.0	8493.0	**0.33**
	D	105.0	3019.0	3773.8	2264.3	8312.0	10390.0	6234.0	0.42
	E1	108.0	4943.0	6178.8	3707.3	10486.0	13107.5	7864.5	0.36
	E2	132.0	6880.0	8600.0	5160.0	13164.0	16455.0	9873.0	0.31
	E3	166.0	4042.0	5052.5	3031.5	9255.0	11568.8	6941.3	0.38
	F	200.0	3061.0	3826.3	2295.8	7927.0	9908.8	5945.3	0.41
	G	229.0	3290.0	4112.5	2467.5	7593.0	9491.3	5694.8	0.38
	H	309.0	3429.0	4286.3	2571.8	8188.0	10235.0	6141.0	0.39
	I	371.0	3092.0	3865.0	2319.0	7686.0	9607.5	5764.5	0.40
	Strawn (MW)	434.0	5546.0	6932.5	4159.5	10627.0	13283.8	7970.3	0.32
Deep Site Profile[2]	Atoka[12]	2636.0	7642.0	10011.0	5273.0	13921.0	18236.5	9605.5	0.28
	Smithwick	4631.0	5557.0	7279.7	3834.3	10894.0	14271.1	7516.9	0.32
	Big Saline[12]	4754.0	10247.0	13423.6	7070.4	18004.0	23585.2	12422.8	0.26
	Marble Falls	4795.0	10520.0	13781.2	7258.8	19740.0	25859.4	13620.6	0.30
	Barnett	5018.0	7783.0	10195.7	5370.3	12858.0	16844.0	8872.0	0.21
	Ellenburger	5265.0	10906.0	14286.9	7525.1	20382.0	26700.4	14063.6	0.30

Table 4. Dynamic properties of subsurface rock materials. Sheet 3 of 4: Additional dynamic properties.

	Unit	Unit Weight[9]		Shear Modulus[10] Mean (ksi)	Minimum C_v for Shear Modulus		G_{max} variation LB	G_{max} variation UB	Damping		
		Wet (pcf)	Dry (pc)		LB	UB	$[G_{max}/(1+C_v)]$ (ksi)	$[G_{max}x(1+C_v)]$ (ksi)	Low Strain D_s Damping[11] (%)	Variation with Strain Relation	Low Strain D_c Damping[13] (%)
	Fill Concrete	150.0	140.0	1495.9	-	-	-	-	-	N/A	-
	Compacted Fill	125.0	-	11.4	-	-	-	-	1.5	Curve 1[16]	0.8
		125.0	-	17.3	-	-	-	-	1.5	Curve 1[16]	0.8
		125.0	-	27.0	-	-	-	-	1.1	Curve 2[16]	0.6
	Fill/Residuum	-	-		-	-	-	-	-	-	-
Shallow Site Profile[1]	A	145.0	135.0	393.7	0.8	0.6	218.7	629.9	1.8	Curve 3[15]	0.9
	B1	135.0	117.0	198.2	0.8	0.6	110.1	317.1	2.0	Curve 4[15]	1.0
	B2	135.0	117.0	214.8	0.8	0.6	119.3	343.7	2.0	Curve 4[15]	1.0
	C	155.0	148.0	1080.4	0.8	0.6	600.2	1728.6	1.8	Curve 3[15]	0.9
	D	135.0	117.0	265.4	0.8	0.6	147.4	424.6	2.0	Curve 4[15]	1.0
	E1	155.0	149.0	816.8	0.8	0.6	453.8	1306.9	1.8	Curve 3[15]	0.9
	E2	155.0	149.0	1582.3	0.8	0.6	879.1	2531.7	1.8	Curve 3[15]	0.9
	E3	150.0	142.0	528.5	0.8	0.6	293.6	845.6	1.8	Curve 3[15]	0.9
	F	130.0	112.0	262.7	0.8	0.6	145.9	420.3	2.0	Curve 4[15]	1.0
	G	135.0	120.0	315.1	0.8	0.6	175.1	504.2	2.0	Curve 5[15]	1.0
	H	140.0	130.0	355.0	0.8	0.6	197.2	568.0	2.0	Curve 4[15]	1.0
	I	145.0	132.0	299.0	0.8	0.6	166.1	478.4	2.0	Curve 5[15]	1.0
	Strawn (MW)	150.0	-	995.0	0.8	0.6	552.8	1592.0	1.8	Curve 2[15]	0.9
Deep Site Profile[2]	Atoka[12]	150.0	-	1890.0	1.0	1.0	945.0	3780.0	1.0	Curve 2[15]	0.5
	Smithwick	150.0	-	1000.0	1.0	1.0	500.0	2000.0	1.0	Curve 2[15]	0.5
	Big Saline[12]	150.0	-	3400.0	1.0	1.0	1700.0	6800.0	1.0	Curve 2[15]	0.5
	Marble Falls	150.0	-	3580.0	1.0	1.0	1790.0	7160.0	0.8	Curve 1[15]	0.4
	Barnett	150.0	-	1960.0	1.0	1.0	980.0	3920.0	1.0	Curve 2[15]	0.5
	Ellenburger	150.0	-	3850.0	1.0	1.0	1925.0	7700.0	0.8	Curve 1[15]	0.4

Table 4. Dynamic properties of subsurface rock materials. Sheet 4 of 4: Notes to Sheets 1–3.

Notes

1.0 Shallow Site Profile derived from site specific data (Ref TXUT-001-FSAR-2.5-CALC-003 andTXUT-001- FSAR-2.5 CALC-004)
2.0 Deep Velocity Profile derived from regional wells as described in the preceeding text
3.0 Depth calculated from the difference between Yard Grade (822 ft MSL (Mean Sea Level)) and the average elevation
4.0 The selected Variability for Velocity is +/- 25% for shallow profile; +/- 50for the compacted fill) ; +/- 31% for deep profile; and +/-500 fps for fill concrete
5.0 Yard Grade is the elevation to which the site will be cut = 822 ft MSL
6.0 Foundation Unit is the top of Layer C on which all critical structures will be founded (either directly or backfilled with concrete)
7.0 Max and Min elevation tops not available for deep site profile, which yielded only one estimate for the top each horizon
8.0 Poisson's Ratio for Shallow Site Profile calculated from Vs and Vp suspension measurements (Ref TXUT-001-FSAR-2.5-CALC-003 and TXUT-001-FSAR-2.5-CALC-004). Deep Site Profile values estimated from deep regional well Vp data as described in the preceeding text
9.0 Unit weight values for Layers A through G estimated based on results of the laboratory tests. Values for Layers H, I, and Strawn (MW) estimated from FSAR Table 2.5.4-5G and based on lithology.
10.0 G_{max} calculated based on suspension Vs or estimated Vs for Deep Site Profile Materials
11.0 Low Strain Damping Ratio in Shear estimated from lithology for Shallow Site Profile through discussion with Dr. Ken Stokoe (Figure A2-2). Deep Site Profile values based on comparison of Vs and lithology of shallow site layers
12.0 Standard deviation in elevation of the top of Big Saline and top Atoka estimated from average standard deviation for other layer elevations
13.0 Damping Ratio in unconstrained compression, D_c should be taken as $0.5D_s$ with a maximum value of 5%.
14.0 Recommended minimum C_v (shear modulus variation factor) values are based on +/- 25% variation in V_s or Min values recommended by DCD (0.5 if test data is available or 1.0 if test data is not available), whichever is higher.
15.0 Curves are assigned from Figure A2-2 in Appendix 2 of this report and were used for the non-linear sensitivity study
16.0 EPRI Curves shown on Figure A2-4b were used for non-linear response of the compacted fill layers

Subnotes (changes based on meeting with WGI and MHI 1-7-08 in Princeton)

A Increase COV for compacted backfill to 50%
B Evaluate increase of compacted backfill Vs as appropriate
C Lower damping % in deep profile to 1.0 for all units except limestone to be kept at 0.8
D Lower damping % to no greater than 2.0 (this is to increase the spectra in the high freq range to lessen the dip of the spectra)
E COV for the shallow profile Vs increased to 25%
F Yard grade changed from 830 to 822

Table 5. Unit weight values.

	Unit Weights Wet Unit Weight (pcf)		
	Avg	Min	Max
Shale	141.6	128.8	161
Limestone	155.3	129.8	164.5
Limestone/Shale	136.7	136.7	136.7
Sandstone	132.7	124.4	140
Soil			
Unit A	151.1	130.2	162.4
Unit B	143.3	128.8	162.9
Unit C	155.1	129.8	164.5
Unit D	143.4	133.1	157.8
Unit E	152.1	135	161.2
Unit F	129.6	124.4	132.5
Unit G	135.8	131	140
Unit H	0	142	142
Unit I	0	0	0

WLA

Boring Location Plan Units 3 & 4

TXU COMANCHE PEAK

Figure 1

Shallow Stratigraphic Profile

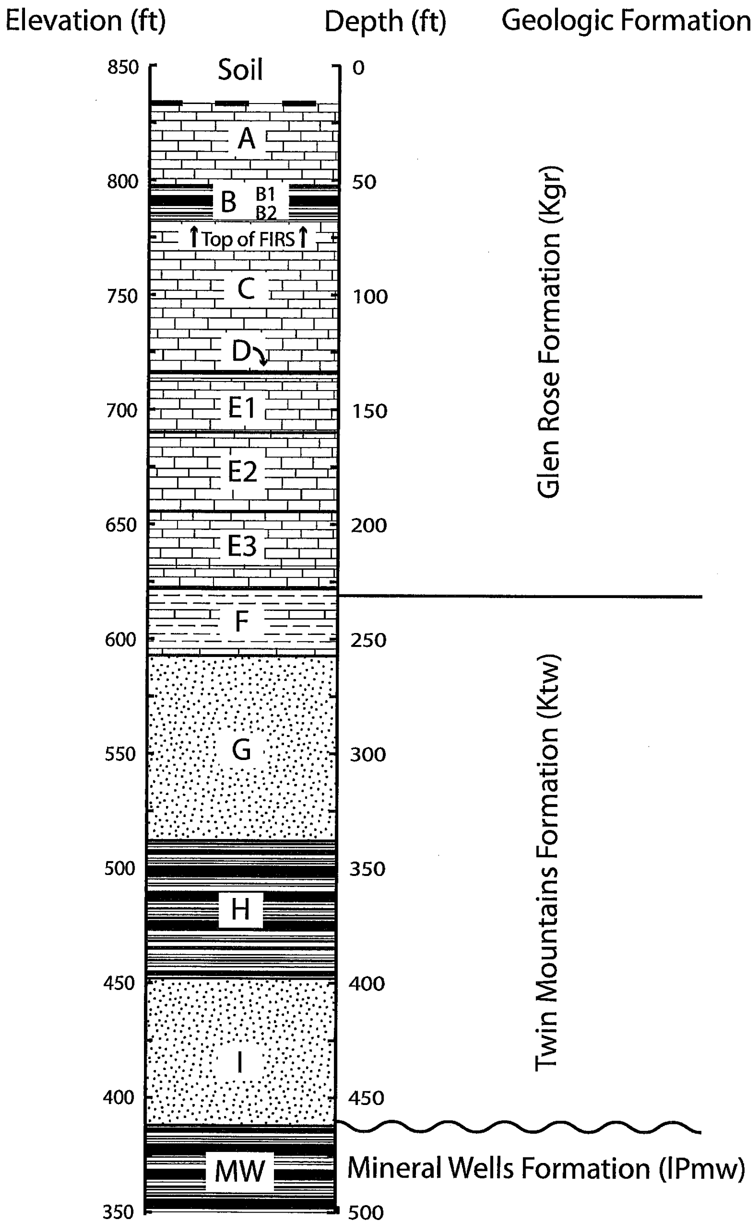

Engineering Unit

A - Limestone with a thicker shale bed at the top and thinner shale beds at the base

B1- Bed of shale with thin interbed of limestone

B2 - Bed of limestone at top dominated with shale at base

C - Massive limestone

D - Two beds of shale with interbed of limestone

E - Massive limestone with subunits E1, E2, and E3 distinguished by changes in resistivity

F - Gradational zone: sandstone, shale, and limestone beds

G - Massive sandstone with interbeds of shale

H - Shale with thin bed of limestone at top and a bed of sandstone at base

I - Massive sandstone with basal conglomerate

MW - Mineral Wells Formation - Shale

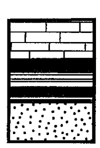

Limestone
Shale
Sandstone
Elevation (830 ft) and Depth (20 ft) of Yard Grade
A   Engineering Unit Symbol

Figure 2

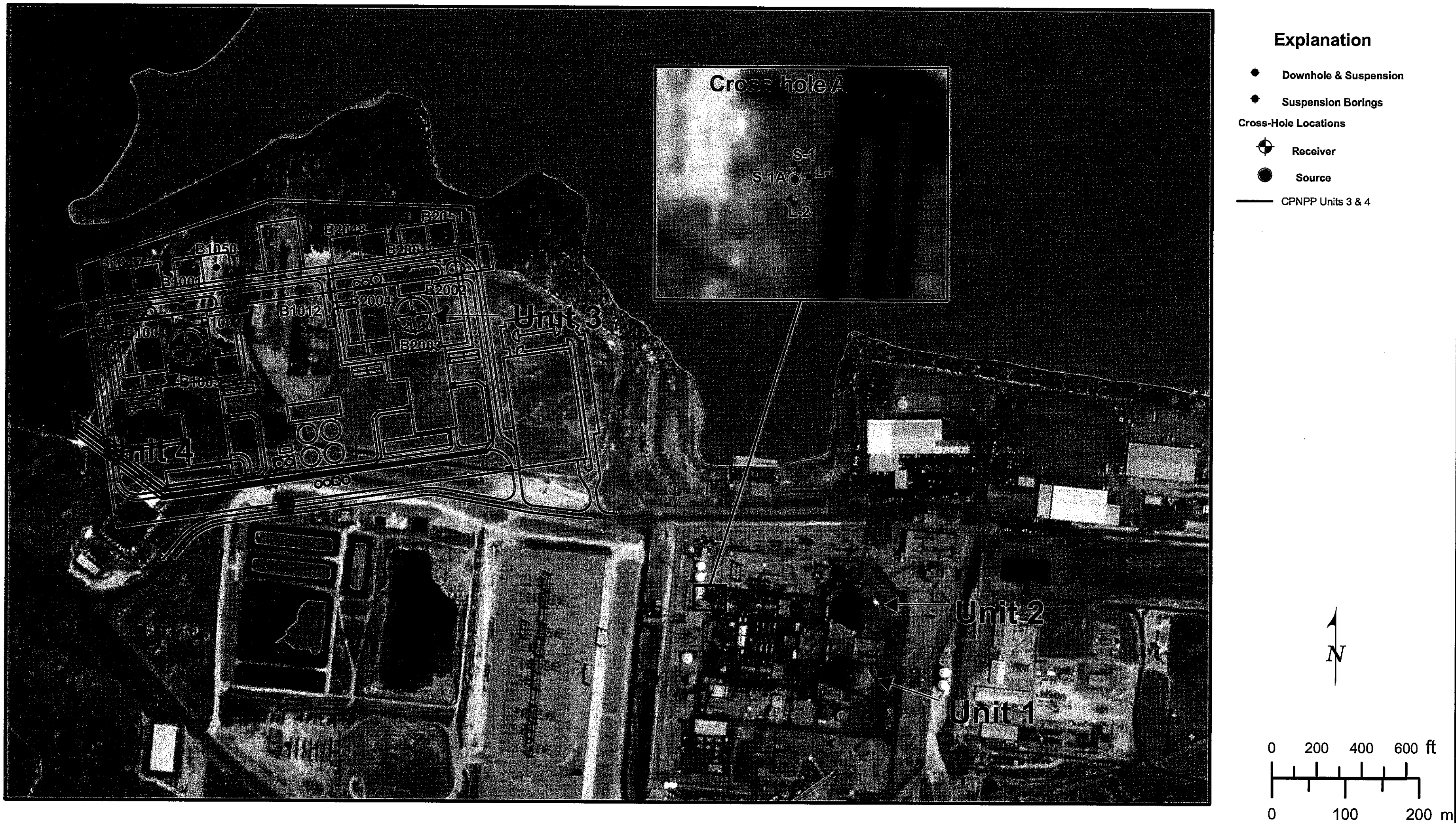

Sources: Building Footprint from WGI DWG file 7/6/07
Aerial photograph - USGS DOQQ false color composite, 1994 - 1997

Projection: NAD83 Texas North Central State Plane Feet

TXU Comanche Peak	
Velocity Data for Units 3 & 4 with Cross-hole Locations from Units 1 & 2	
WLA William Lettis & Associates, Inc.	Figure 3

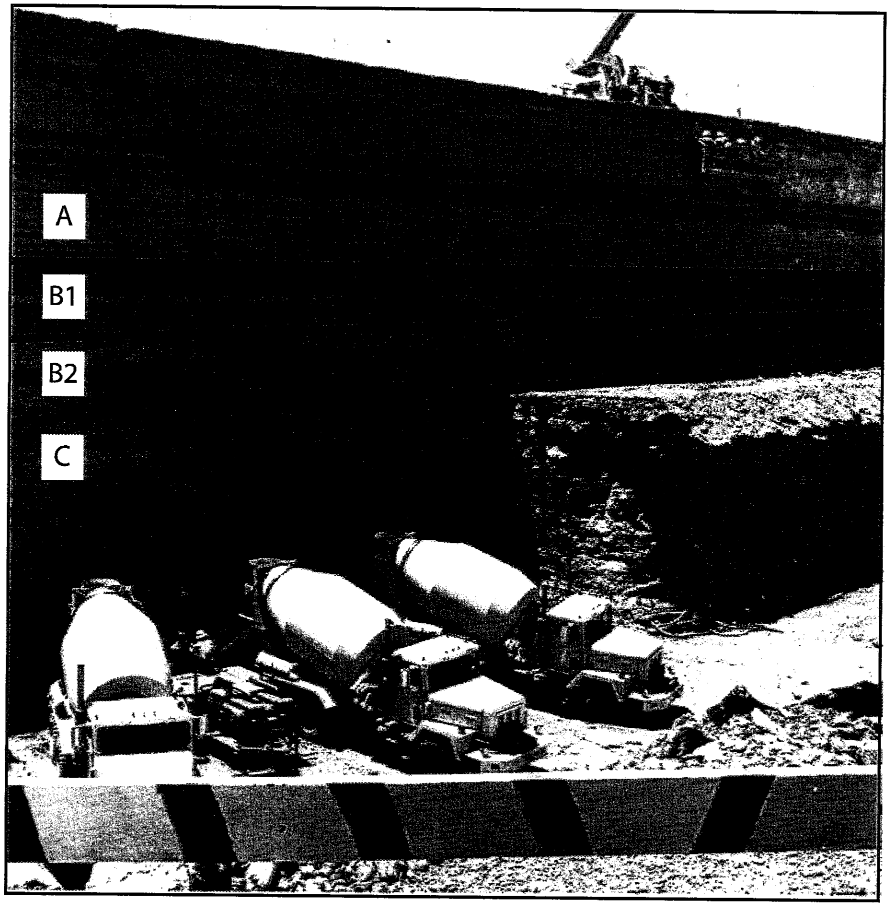

NUMBER 87
AUGUST 8, 1975

TEXAS UTILITIES SERVICES, INC.
COMANCHE PEAK STEAM ELECTRIC STATION
1980-82 2300 MW INSTALLATION

TURBINE GENERATOR AREA. BOTTOM–PUMPING CONCRETE INTO UNIT 1 CIRCULATING WATER DISCHARGE TUNNEL; TOP–SCALING SOUTH EXCAVATION WALL. VIEW TO SOUTHWEST

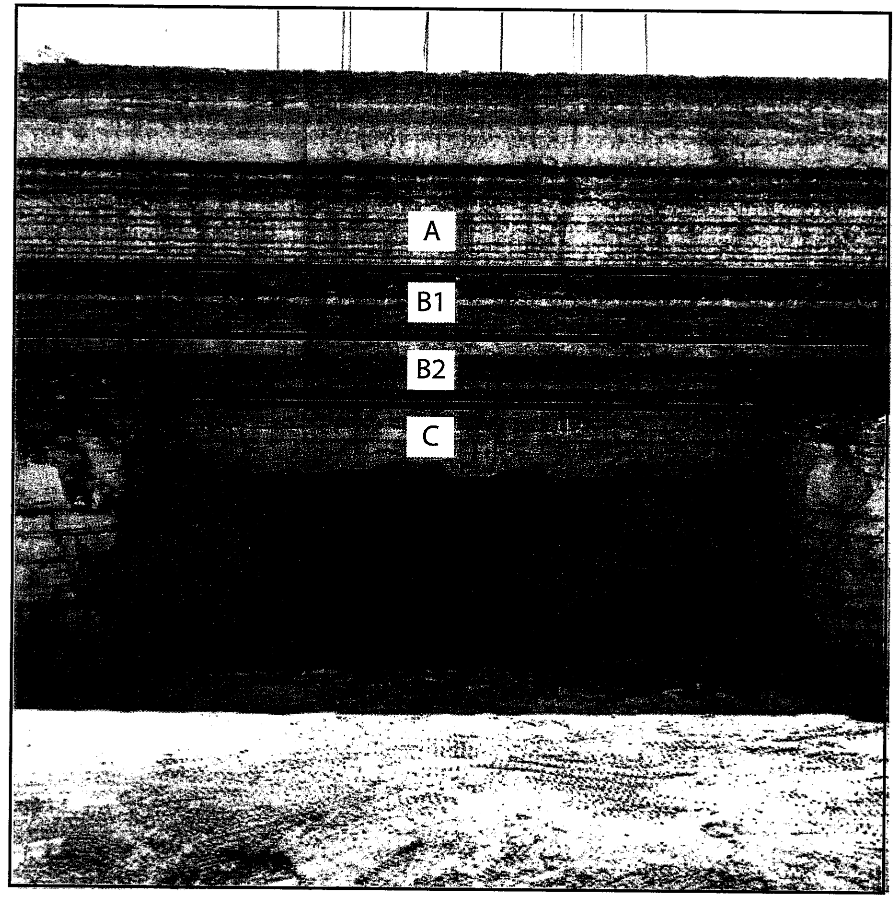

NUMBER 101
SEPTEMBER 22, 1975

TEXAS UTILITIES SERVICES, INC.
COMANCHE PEAK STEAM ELECTRIC STATION
1980-82 2300 MW INSTALLATION

UNIT 1 TURBINE DISCHARGE WATERBOX OVERHANG EXCAVATION. VIEW TO SOUTH

Figure 4 CP Units 1 & 2 excavation photos with interpreted Units 3 & 4 Engineering Stratigraphy (see Fig. 2)

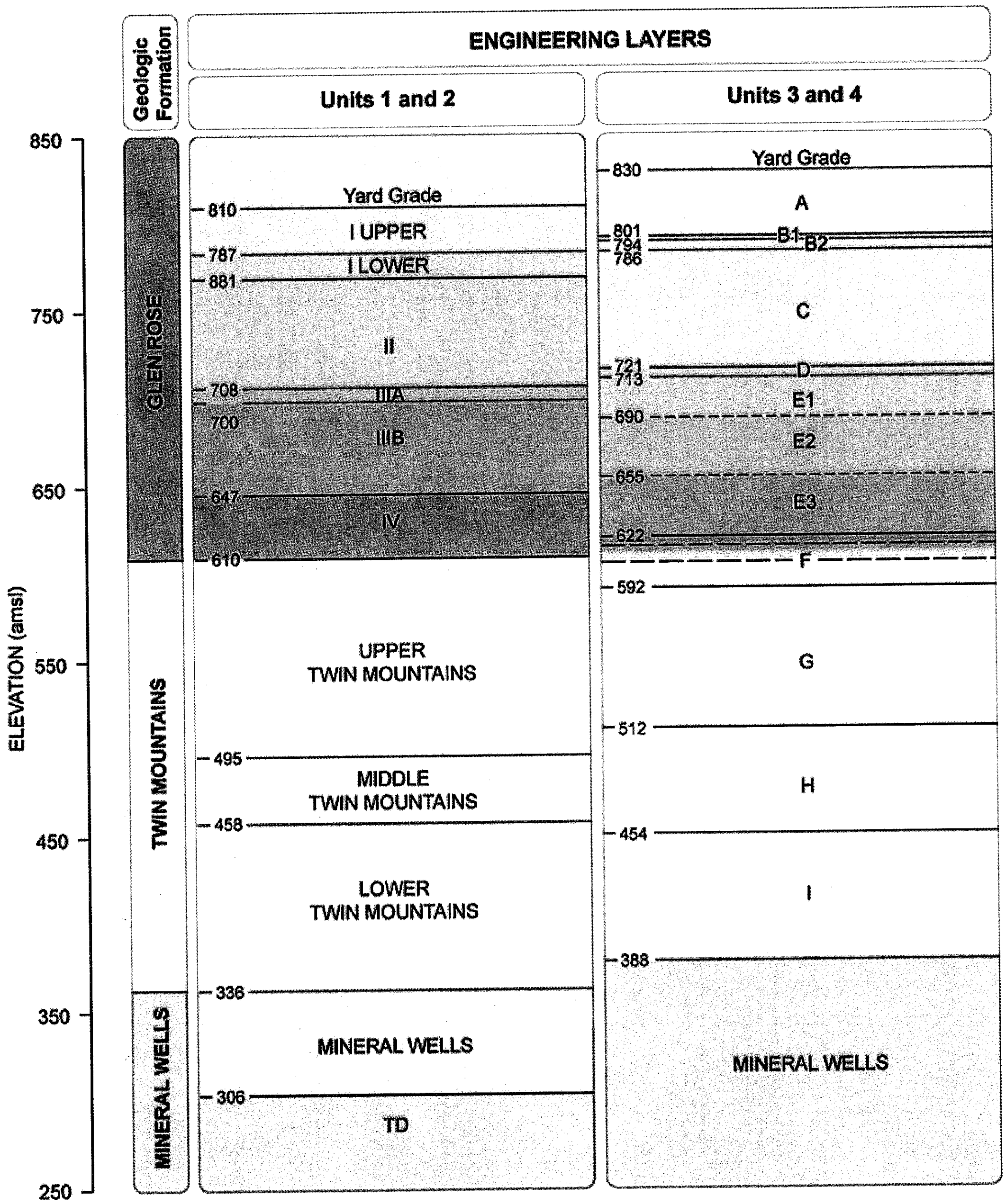

Comparison of Engineering Stratigraphy

Figure 5

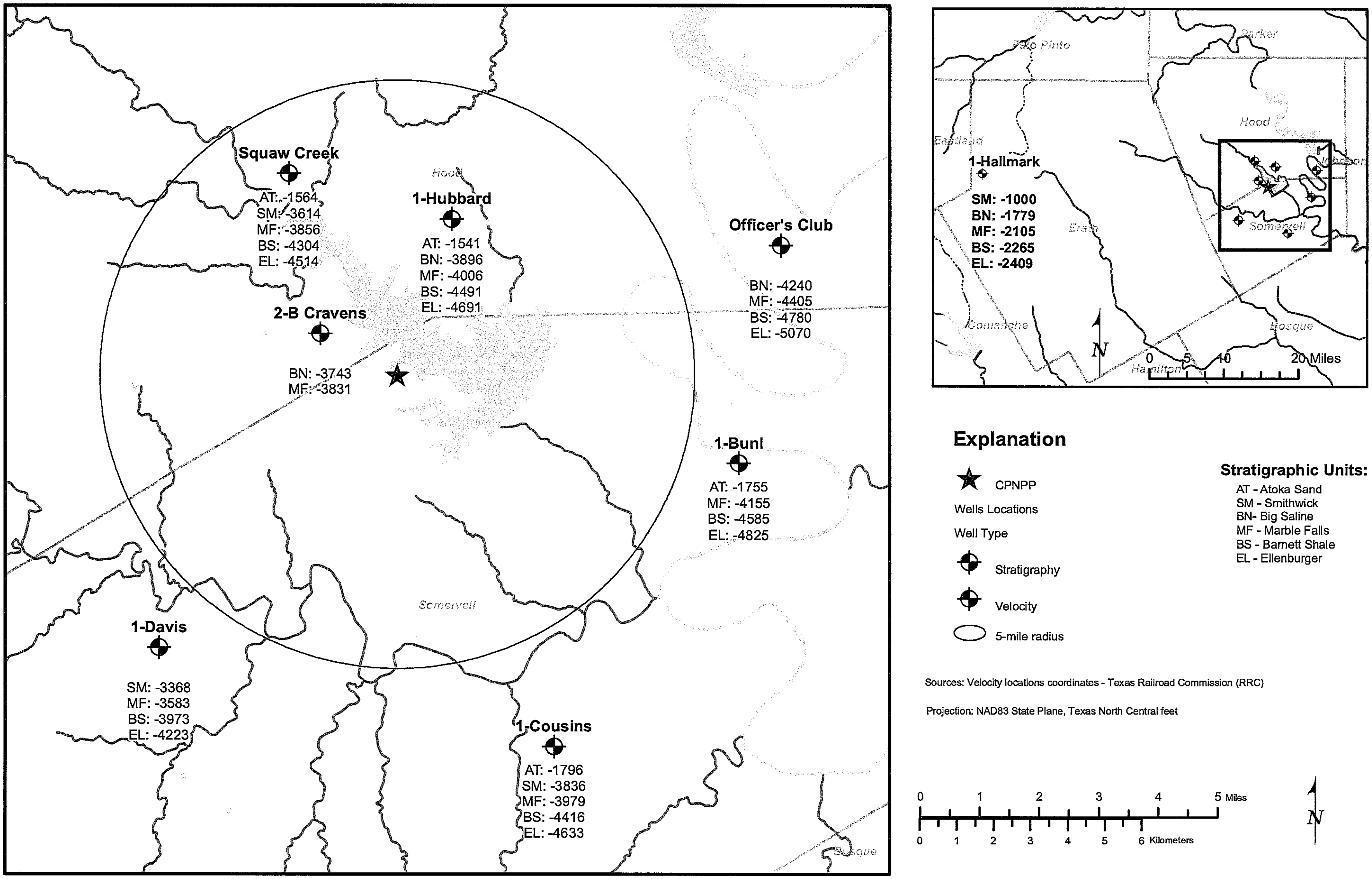

WLA

Map of Well Data Used for Deep Stratigraphy Velocity Profile

TXU COMANCHE PEAK

Figure 6

Well Vp Data

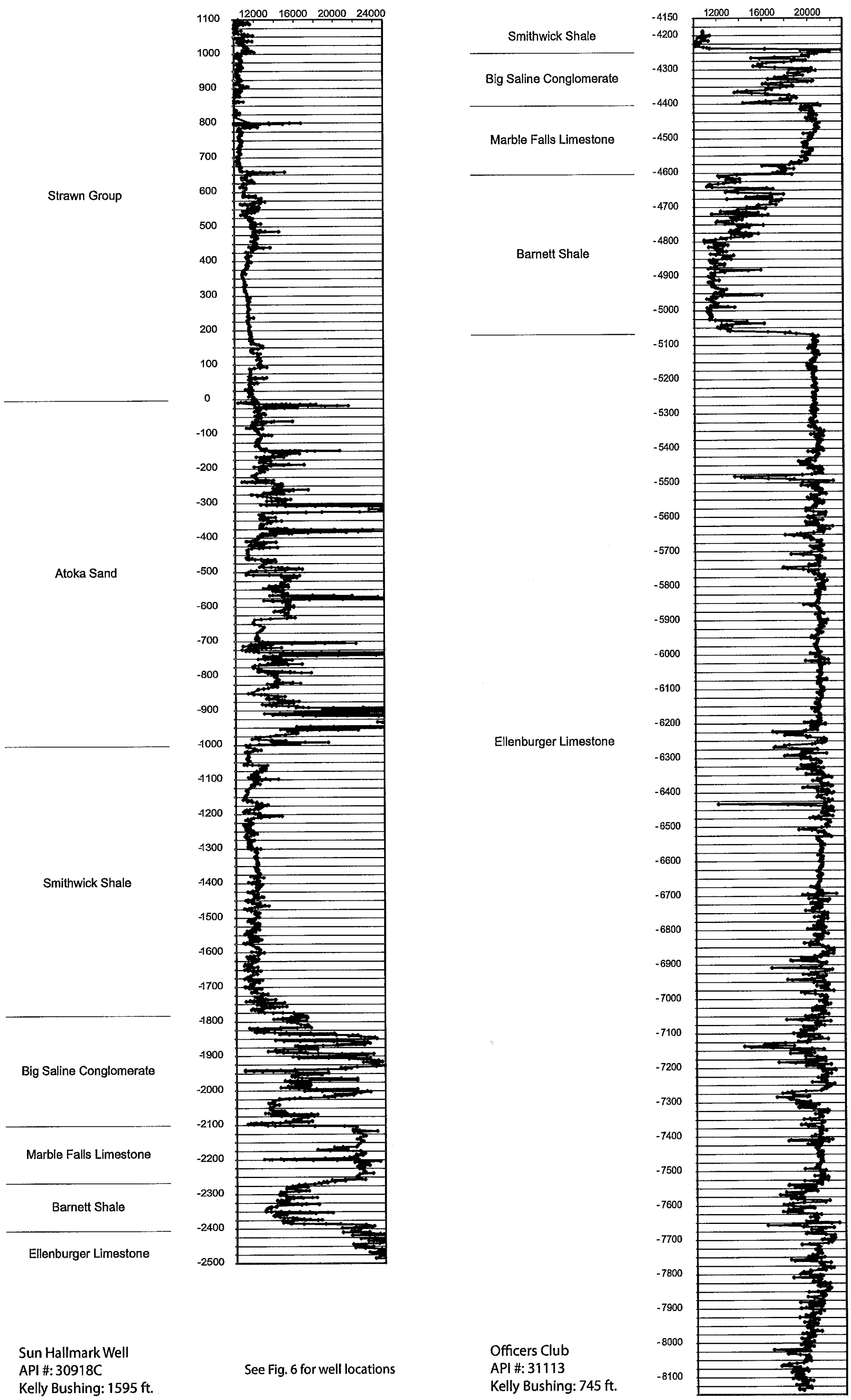

Figure 7

Shallow Velocity Profile -- Regression

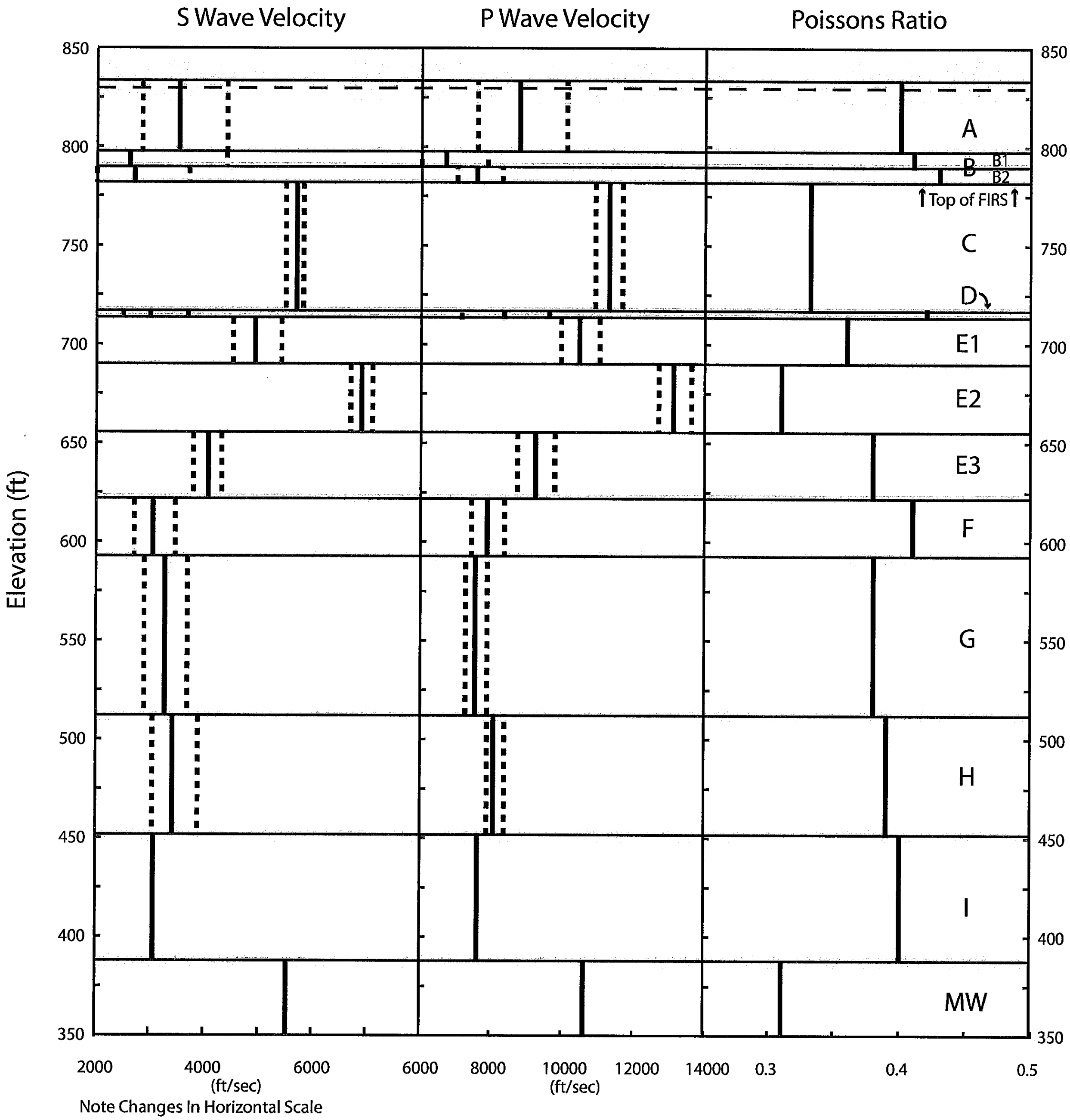

(dotted/solid bars)	Mean value and 2σ, when available
(solid line)	Unit top and standard deviation
(dashed line)	Elevation of Yard Grade
A	Engineering Unit Symbol (see Fig. 2 for Unit descriptions)

Figure 8

WLA

T X U C O M A N C H E P E A K

Suspension, Downhole, & SASW Log Locations Units 3 & 4

Figure 9

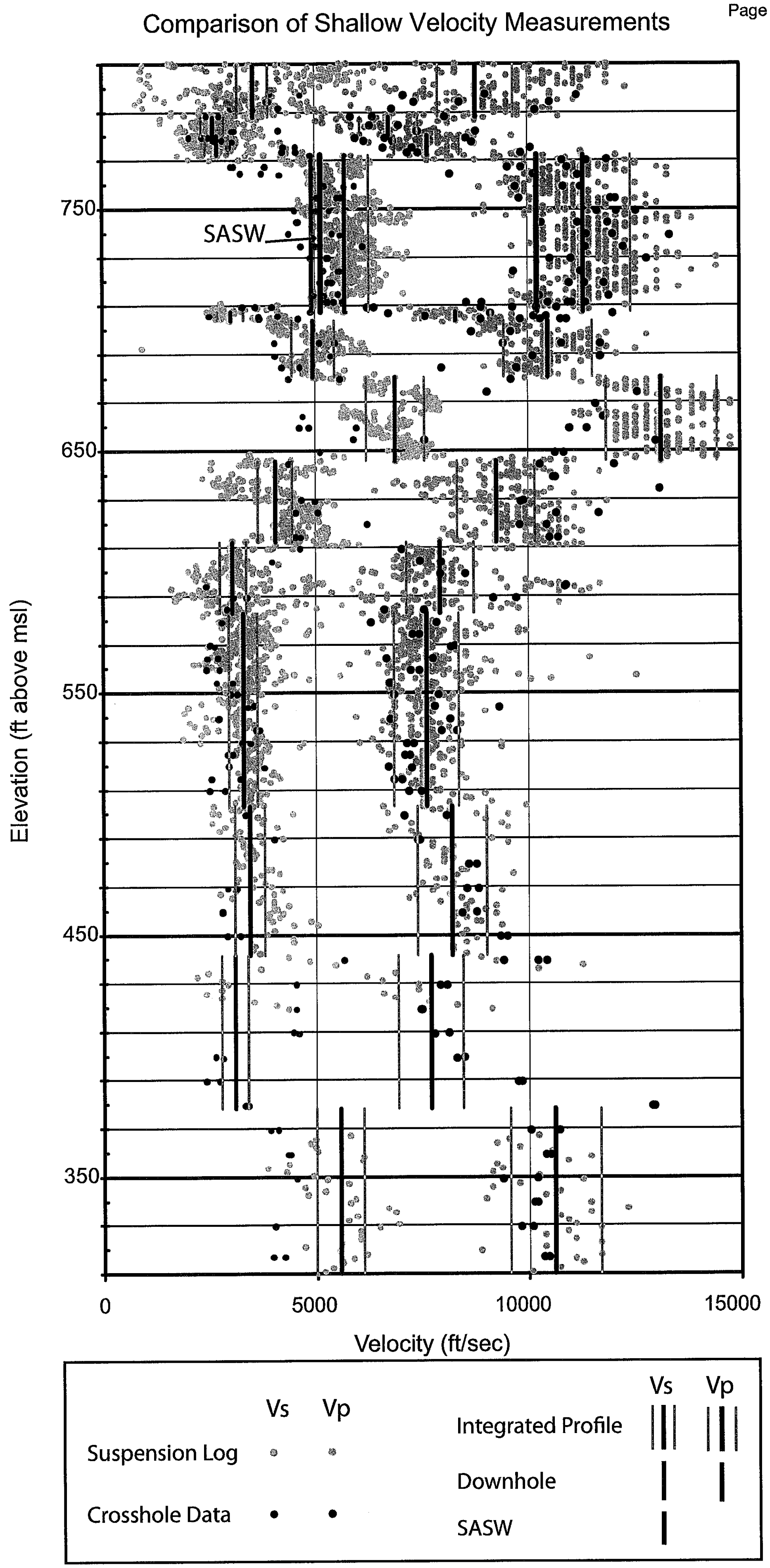
Comparison of Shallow Velocity Measurements
SASW
750
650
550
450
350
Elevation (ft above msl)
0
5000
10000
15000
Velocity (ft/sec)
Vs
Vp
Suspension Log
Crosshole Data
Integrated Profile
Downhole
SASW

Figure 10

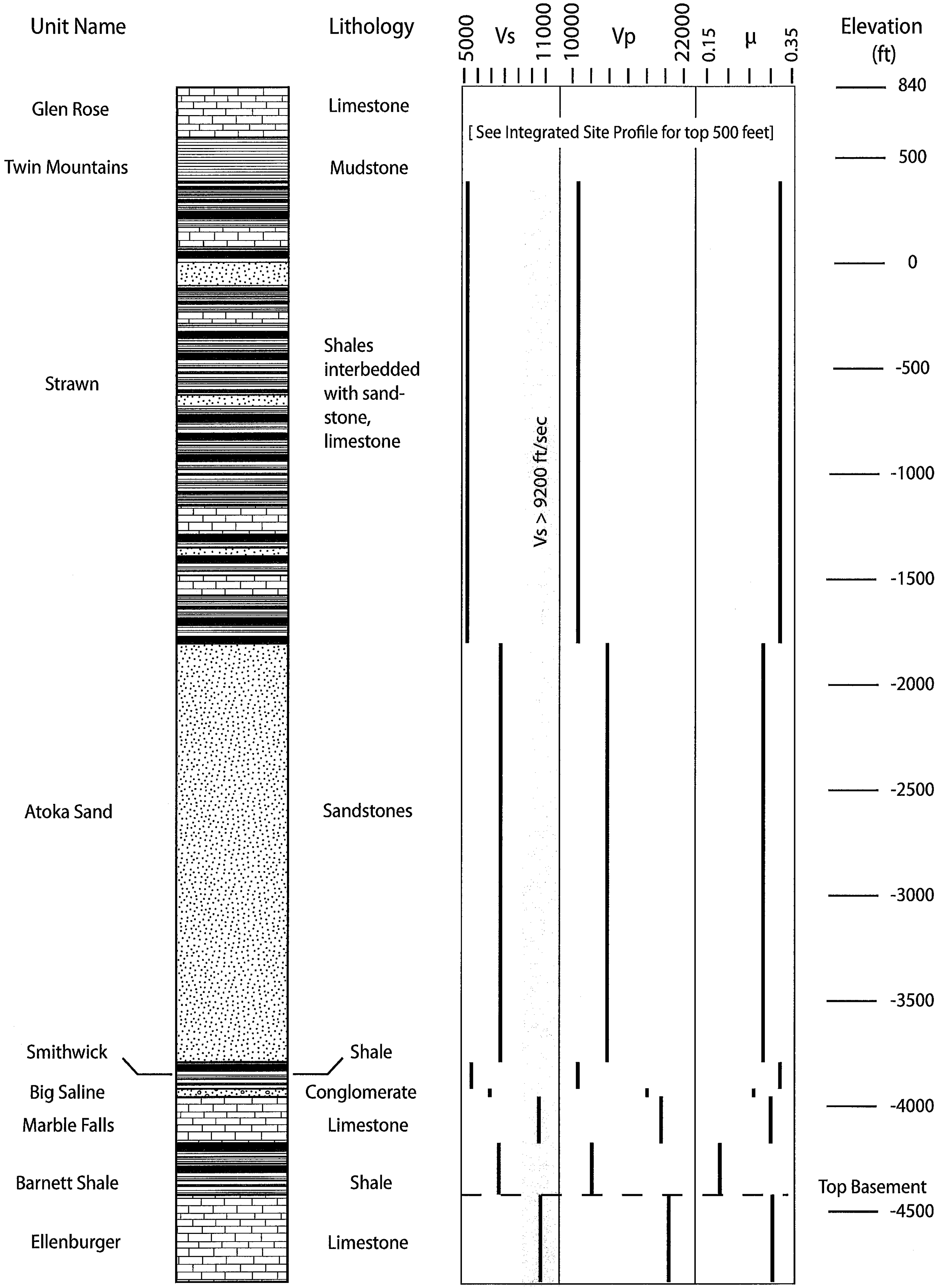
Unit Name
Lithology
5000
Vs
11000
10000
Vp
22000
0.15
μ
0.35
Elevation (ft)
840
500
0
-500
-1000
-1500
-2000
-2500
-3000
-3500
-4000
-4500
Glen Rose
Limestone
[See Integrated Site Profile for top 500 feet]
Twin Mountains
Mudstone
Strawn
Shales interbedded with sand-stone, limestone
Vs > 9200 ft/sec
Atoka Sand
Sandstones
Smithwick
Shale
Big Saline
Conglomerate
Marble Falls
Limestone
Barnett Shale
Shale
Top Basement
Ellenburger
Limestone

Figure 11

APPENDIX 1
Calculation of V_s for Atoka Unit

Unit	V_p	V_s
Mineral Wells	10485	5406
Smithwick	10894	5557
Big Saline	18004	10247
Marble Falls	19740	10520
Barnett	12118	7620
Ellenburger	20382	10906
Atoka	13921	7642

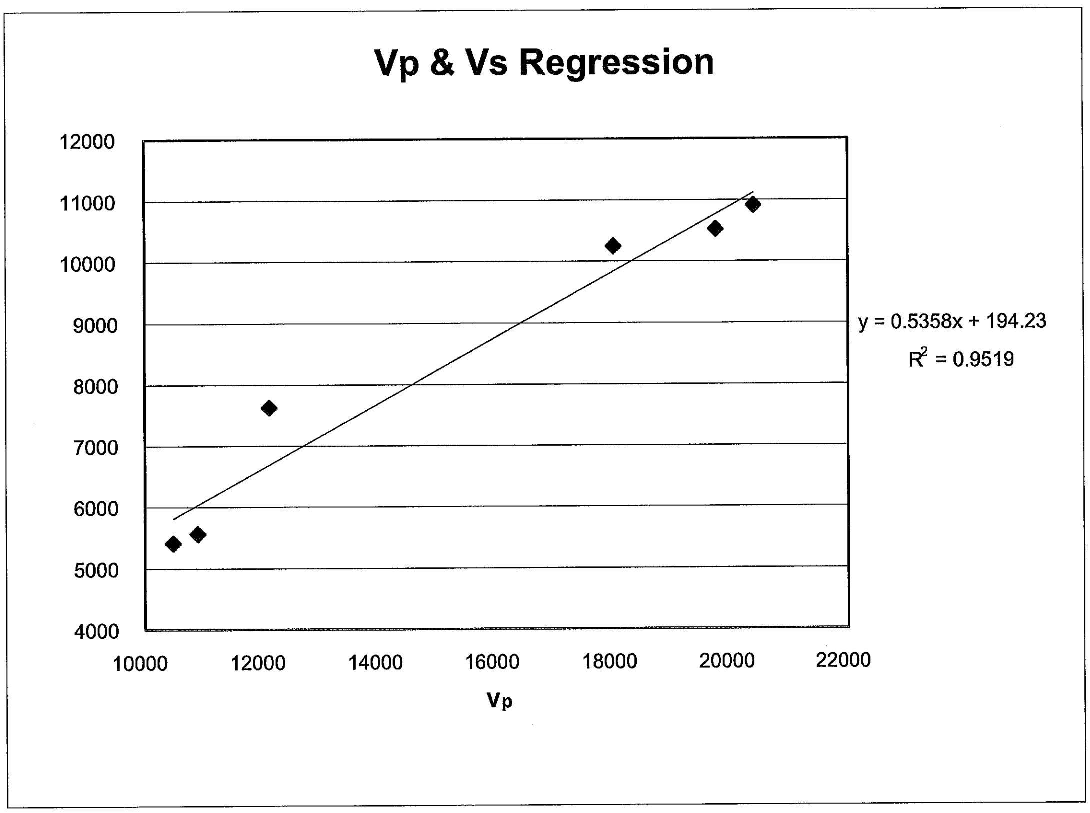

APPENDIX 2

Non-Linear Sensitivity Analysis

Non-linear Sensitivity Analysis

Overview

Site-specific and regional data indicate that the CPNPP site is underlain by a sequence of limestones, shales and sandstones with shear wave (Vs) velocities greater than about 5800 feet/sec. Because these velocities are about half of what would be measured for crystalline rock yet more than double than a typical soil site, the profile was tested for sensitivity to non-linear behavior.

Using shear wave velocity, rock lithology (limestone, shale and sandstone) and depth as discriminators, shear modulus (G/Gmax) and damping ratio (D) versus shear strain relationships were developed through consultation with Dr. Ken Stokoe, Professor University of Texas. These properties as summarized in Table 4 above and shown on Figures A2-1 and A2-2 were then used to generate a test case to compare the strains to a profile where the properties were assumed to behave linearly.

Estimation of Strain Dependent Properties

The profile was divided into lithologies within the upper 400 feet and those deeper than 400 feet to account for increasing confining stress and unit weight. The following relationships were determined with corresponding minimum damping ratio (D_{min}) defined:

Figure A2-1 and A2-2 Curve	Material and Properties	Shear Strain %	G/G_{max}	D %
1	Deep Limestone (Depth > 400 ft)	0.0001	1.000	0.800
		0.0010	1.000	0.800
		0.0030	0.990	0.900
		0.0100	0.980	1.100
		0.0300	0.940	1.600
2	Deep Shale & Sandstone (Depth >400 ft)	0.0001	1.000	1.800
		0.0002	1.000	1.800
		0.0005	1.000	1.800
		0.0010	0.990	1.900
		0.0020	0.985	2.000
		0.0050	0.980	2.200
		0.0100	0.960	2.400
		0.0200	0.910	3.000

3	Shallow Limestone (Depth <400 ft)	0.0001	1.000	1.800
		0.0002	1.000	1.800
		0.0005	1.000	1.800
		0.0010	0.990	1.900
		0.0020	0.985	2.000
		0.0050	0.980	2.200
		0.0100	0.960	2.400
		0.0200	0.910	3.000
4	Shallow Shale (Depth <400 ft)	0.0001	1.000	3.200
		0.0002	1.000	3.200
		0.0005	0.980	3.500
		0.0010	0.950	3.800
		0.0020	0.900	4.200
		0.0050	0.820	5.100
		0.0100	0.730	6.200
		0.0200	0.620	7.600
5	Shallow Sandstone (Depth <400 ft)	0.0001	1.000	2.500
		0.0002	1.000	2.500
		0.0005	0.990	2.600
		0.0010	0.980	2.700
		0.0020	0.950	2.900
		0.0050	0.910	3.200
		0.0100	0.850	4.000
		0.0200	0.770	5.000

Calculations

Site-response calculations were performed using an equivalent-linear formulation and, using as rock input the 10^{-4} broadband spectrum from the probabilistic seismic hazard analysis, and considering a profile that extends from bedrock to Elevation 782 feet (top of Glen Rose Limestone Layer C). Calculations were performed for two separate cases, as follows: (1) a linear analysis, using the low-strain damping ratios from Table 4; and (2) a non-linear analysis, using the strain-dependent damping and stiffness properties given in Figures A2-1 and A2-2 and tabulated above.

Results

Figures A2-3 compares the spectra at the top of the profile, for the two sets of calculations. The linear results are slightly higher than the non-linear results. This is which is attributed mainly to the conscious conservative choice of damping ratios for the linear analysis (see Table 4, subnotes C and D). An additional contributor is the increased damping that accompanies nonlinear deformation.

Appendix 2 References
Risk Engineering, Inc. (2007). *High frequency and low frequency horizontal rock spectra,* REI QA record 0737-ACR-026.

Risk Engineering, Inc. (2008). *Calculation of Site Response for Comanche Peak Units 2 and 3, Rev. 1.* REI QA record 0737-ACR-030.

Figure A2-1: G/G_{max} vs. Strain for Rock Materials

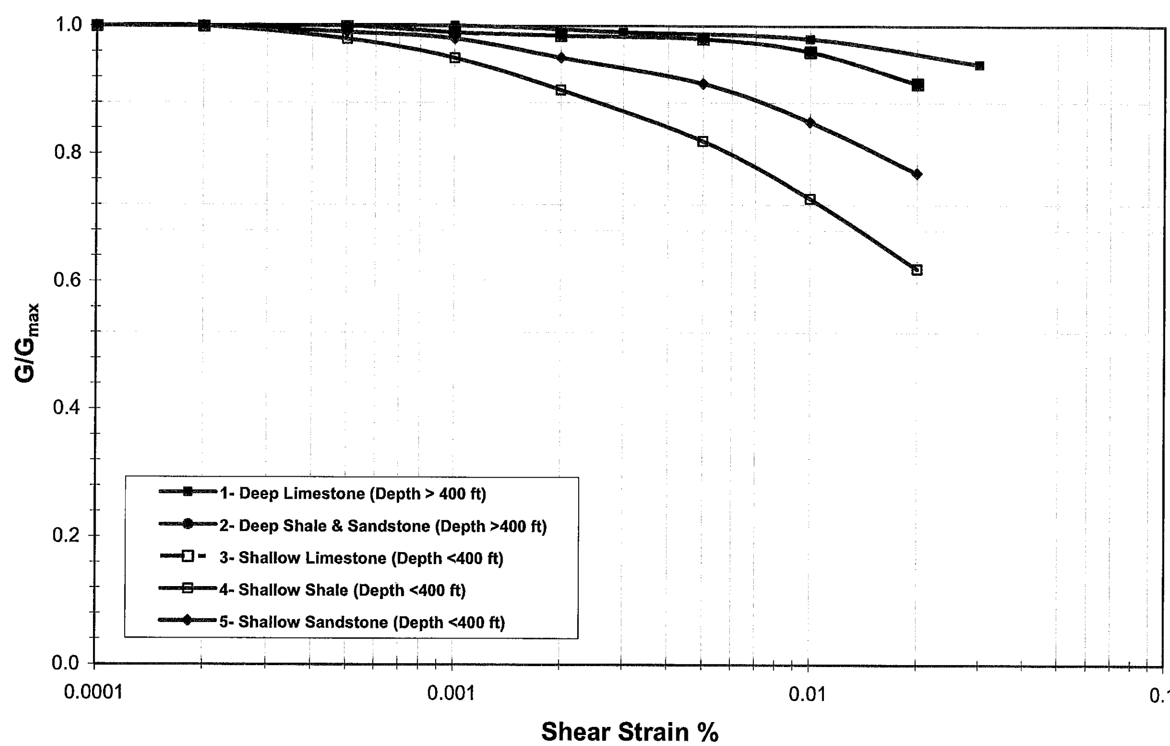

Figure A2-2: Damping in Shear vs. Strain for Rock Materials

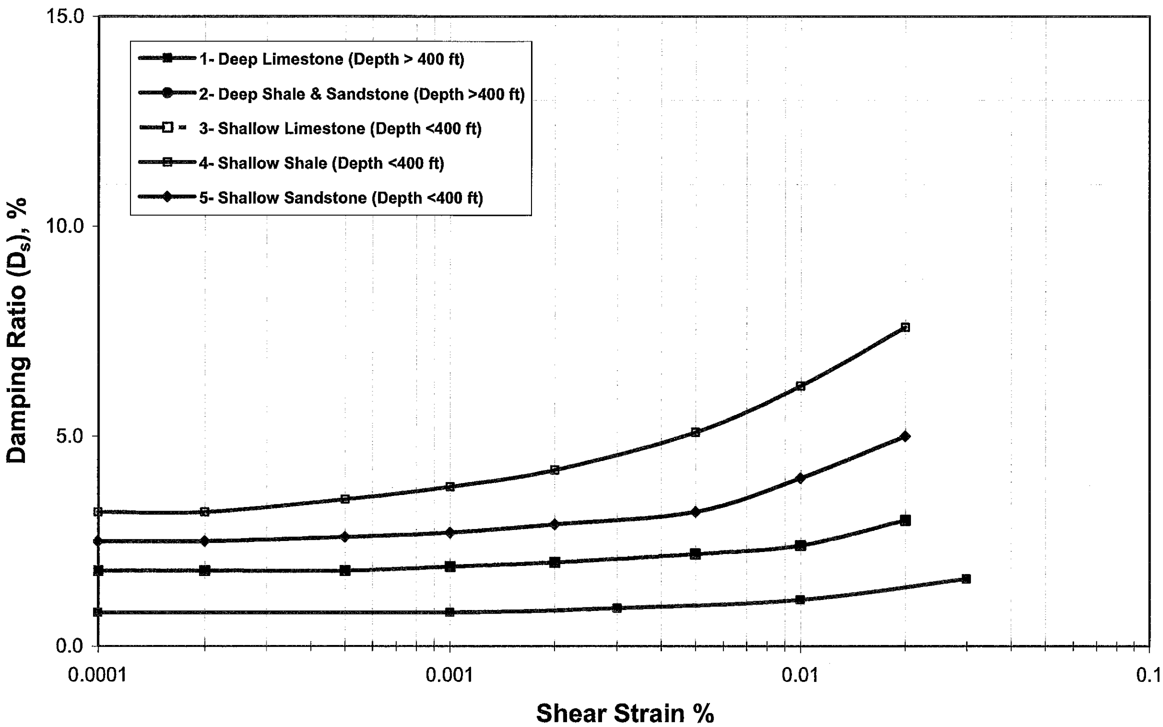

Figure A2-3: 1E-4 Broadband Linear vs. Nonlinear Median Soil Spectra

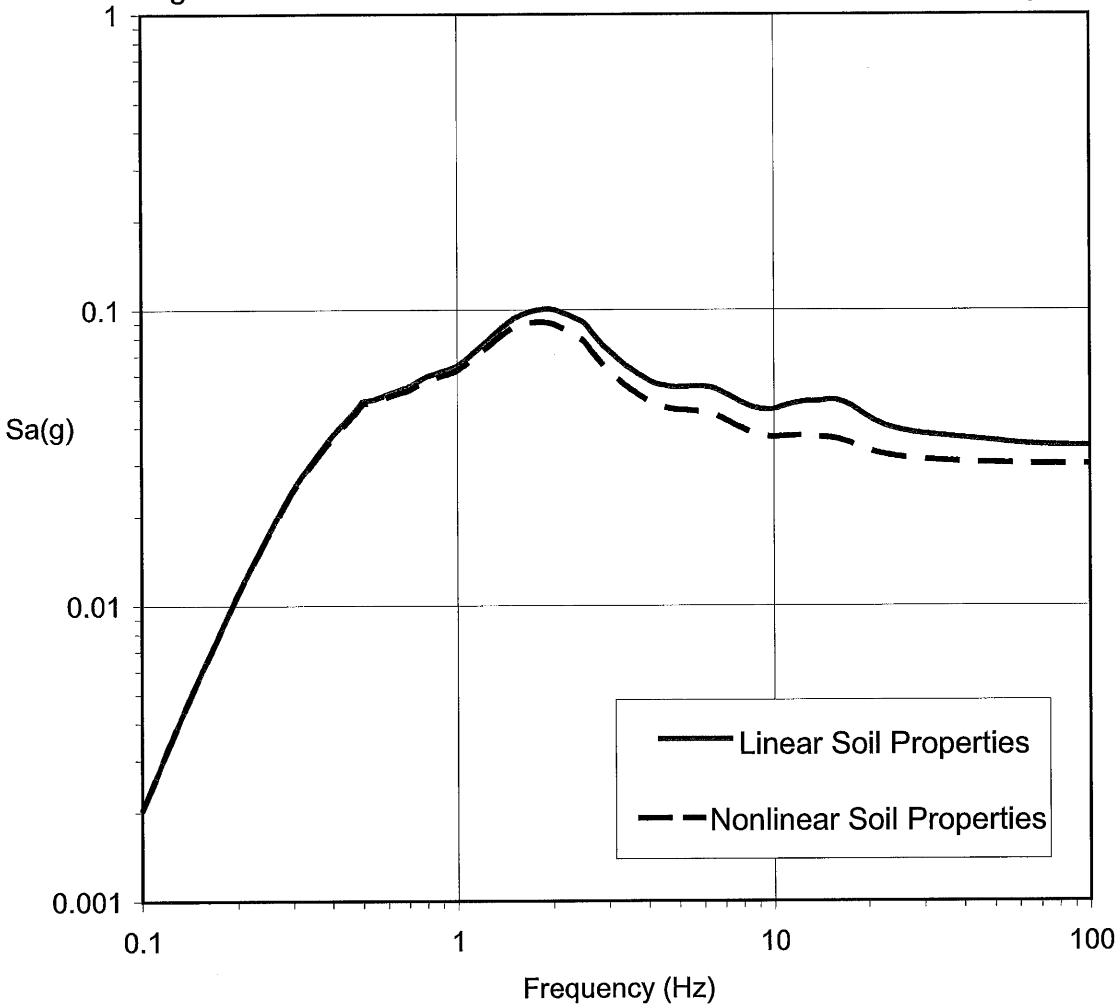

Figure A2-4a: G/G_{max} vs. Strain (Sand Characteristic Behaviour, EPRI 1993)

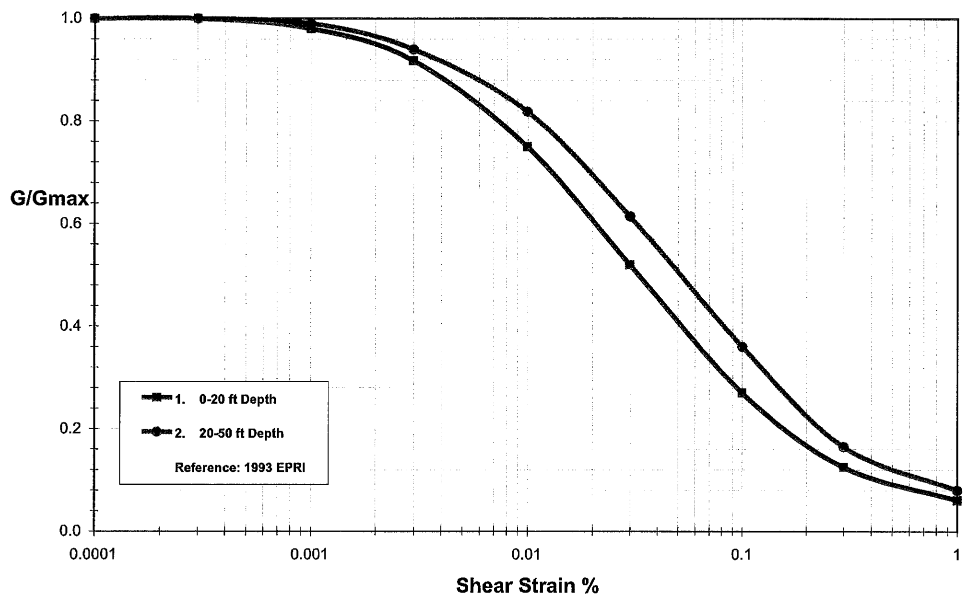

Figure A2-4b: Damping in Shear vs. Strain (Sand Characteristic Behaviour, EPRI 1993)

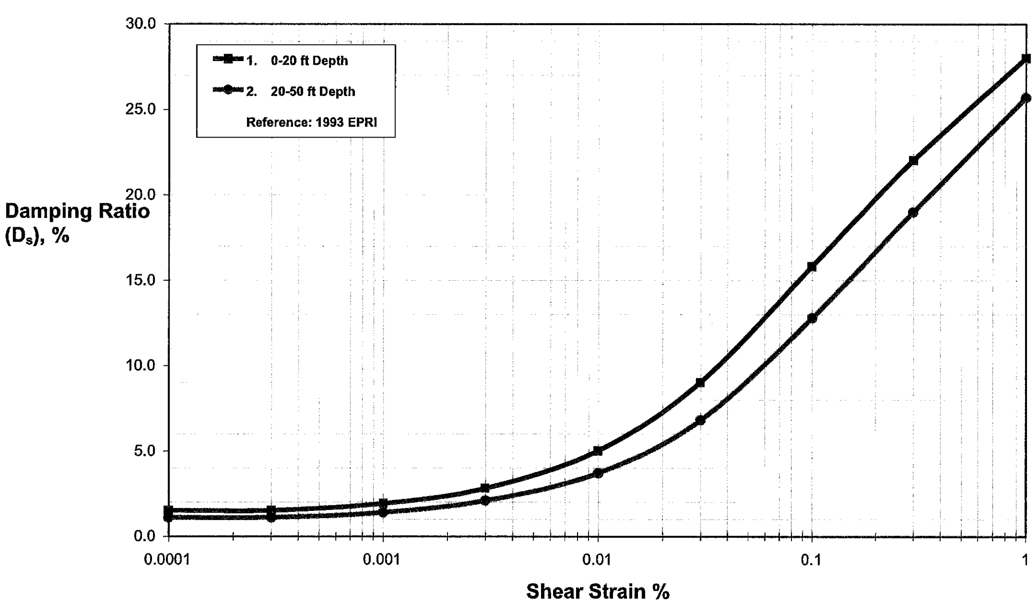

APPENDIX 3

Site Response Sensitivity Analysis

Overview

Because all Category 1 structures will be founded directly on Layer C or a leveling fill concrete, the top of Layer C was also defined as the Foundation Input Response Spectra depth (FIRS1) hence, GMRS/FIRS1. The following sensitivity analyses have been developed for the site-specific profile GMRS/FIRS1 to first test the relationship assigned between the layers defining the shallow and deep profile. Next, the computational procedure is tested by following guidance within Interim Staff Guidance, on Ensuring Hazard Consistent Seismic Input for Site Response and Soil Structure Interaction Analyses, DC/COL, ISG-017 and assuming non-linearity of the shallow profile. Last, an alternative model for Layer C will be evaluated by including shale interbedding with non-linear properties.

Sensitivity Run 1 Approach

Sensitivity analysis 1 uses full correlation between all layers in developing the randomized site profiles, in contrast to the randomized profiles presented in the FSAR that use a partial correlation for the shallow profile layers.

The site-response calculations in FSAR Section 2.5 utilize 60 randomized profiles in order to characterize uncertainty in the dynamical properties of the soil column and the effect of these uncertainties on site response. In this randomization, the correlation coefficient between ln[Vs] (the natural logarithm of the shear-wave velocity) values in adjacent layers of the profile is given a value between 0 and 1, which varies as a function of depth and layer thickness, based on a statistical analysis of profiles at many sites with similar soil characteristics (Toro, 1996; see also EPRI, 1993, Risk Engineering, 2005). This choice of correlation coefficients represents standard practice and has been used in other COLA applications.

The uncertainty used in the randomization for ln[Vs] in the deep profile (i.e., coefficient of variation of 0.35) is consistent with the data available for the local geology, and its associated uncertainty. This variation, coupled with the assumption of full Vs correlation, is equivalent to using alternative discrete models for the deep profile. Therefore, one can also use the results from Run 1 to test the sensitivity to the use of alternative deep profiles.

The steps for sensitivity run 1 include the following.

1. Generate a new set of 60 randomized profiles for the GMRS horizon, using a ln[Vs] correlation coefficient of 1 at all depths, and keeping all other input parameters at the same values.
2. Perform site-response calculations for the 1E-5/year broadband rock motions, considering these 60 randomized profiles.
3. Calculate summary statistics (median and logarithmic standard deviation) on the amplification factors for all frequencies of interest.
4. Compare these summary statistics to those obtained in the original calculations for Section 2.5 of the FSAR.

Sensitivity Run 1 Results

Figures A3-1 and A3-2 show the 60 randomized profiles (entire depth, and top portion, respectively). Unlike the profiles used in FSAR Section 2.5, a profile is consistently high or consistently low over the entire depth of the soil column.

Figure A3-3 compares the summary statistics of the computed amplification factors to those used in FSAR Section 2.5 (identified as Original COLA). The logarithmic-mean amplification factors are essentially identical. The standard deviations differ somewhat. These differences are not large, and they do not show a definite pattern. Given the small extent of these differences, and the fact that the model of partial-correlation model for Vs is more credible than the full-correlation model, it is concluded that the amplification factors in FSAR Section 2.5 are adequate.

Sensitivity Run 2 Approach

Sensitivity analysis 2 utilizes the non-linear degradation curves developed in Appendix 2 of this report and will also consider full correlation between layers.

The site-response calculations in FSAR Section 2.5 of the FSAR assumed linear (i.e., strain-independent) behavior of the soils in the shallow portion of the profile (Layers A through I, plus the Strawn formation), on the basis of the low strains that were anticipated for the rock motions at the site. As part of a previous the sensitivity analysis, strain-dependent modulus-reduction and damping curves were developed and are documented in Appendix 2, but were not used in the calculations because the resulting amplification factors were slightly lower than those from linear analyses. The motivation for sensitivity analysis 2 is to test the sensitivity of the amplification factors to using the site response methodology of draft ISG-017 instead of that outlined in FSAR Section 2.5.2. The ISG-017 methodology leads to higher strains because it considers the dynamic strains induced by soil deposits located above the plant foundation.

The steps for sensitivity run 2 include the following.

1. Generate a new set of 60 randomized profiles for a soil column that extends to plant grade, including strain-dependent shear modulus and damping for the shallow profile. Use a ln[Vs] correlation coefficient of 1 at all depths.
2. Perform site-response calculations for the 1E-5/year broadband rock motions, considering these 60 randomized profiles. For this calculation, calculate the amplification factors at the GMRS horizon by following the two-step approach contained in the NEI White Paper, *Consistent Site Response – SSI Calculations*. and accepted by ISG-017 for embedded structures that are analyzed as surface structures.
3. Calculate summary statistics (median and logarithmic standard deviation) on the amplification factors for all frequencies of interest).
4. Compare these summary statistics to those obtained in the original calculations for Section 2.5 of the FSAR.

Sensitivity Run 2 Results

Figure A3-4 shows the peak strains as a function of depth for the 60 randomized profiles. The higher strains occur in the 200-370 feet depth range, with a logarithmic-mean value slightly below 0.01%. This depth range includes limestones, sandstones, and shales, with shear-wave velocities near 3200 feet/second. Recalling Figures A2-1 and A2-2, we note that the behavior of these strata is nearly linear, except for the 62 feet of shale (Layer H),

Figure A3-5 compares the summary statistics of the computed amplification factors to those used in FSAR Section 2.5 (identified as Original COLA). At frequencies above 1 Hz, the logarithmic-mean amplification factors are 10 to 20% lower for the nonlinear runs that for Section 2.5. The standard deviations differ somewhat. As was the case in Figure A3-3, these differences are not large, and they do not show a definite pattern. Figure A3-6 compares the results from Run 1 and Run 2, in order to isolate the effects of nonlinearity from the effects of full Vs correlation. This comparison shows the same reduction in median amplification factors and a slight increase in the standard deviations.

Given the above comparisons, it is concluded that the amplification factors in FSAR Section 2.5 are adequate.

Sensitivity Run 3 Approach

The third sensitivity analysis considers the effect of interbedded shale layers within the foundation bearing Layer C. As in Run2, Run 3 considers the effect of soil nonlinearity and follows the methodology in draft document ISG-017. These shale layers are modeled as nonlinear, with appropriate degradation properties.

The steps for sensitivity run 3 include the following.

1. Develop a model for the location, extent, and dynamic properties of the interbedded shale within Layer C, including low-strain properties and degradation curves.
2. Generate a new set of 60 randomized profiles for the GMRS horizon, including shale interbeds within Layer C, and including strain-dependent shear modulus and damping for the shallow profile. Use a ln[Vs] correlation coefficient of 1 at all depths
3. Perform site-response calculations for the 1E-5/year broadband rock motions, considering these 60 randomized profiles. For this calculation, follow the two-step approach contained in the NEI White Paper and recommended by ISG-017 for embedded structures that are analyzed as surface structures.
4. Calculate summary statistics (median and logarithmic standard deviation) on the amplification factors for all frequencies of interest).
5. Compare these summary statistics to those obtained in the original calculations for Section 2.5 of the FSAR.

Interbedded Layer C Model Development

The category 1 structures are to be founded directly on engineering Layer C which is characterized as a 60 feet thick limestone with a mean shear wave velocity of about 5800 feet/sec. Lying above Layer C are Layers A and B which will be excavated/removed. The uniformity of Layer C has been determined from the review of over 114 geotechnical core borings drilled beneath the CPNPP Units 3 and 4 including a re-evaluation of the boring logs and lithologic descriptions, geophysical measurements and laboratory test results.

Review of Core Lithologic Descriptions and Photographs

The vertical and lateral distribution of shale within Layer C was quantified from a detailed review of each boring log to asses both the total cumulative percentage of shale as well as the lateral continuity of shale layers between borings. During the review of the core boring descriptions and photographs for layer C, four distinct rock lithologies were classified as "shale":

- *Shale* – indicated as having little to no reaction with HCl and signs of dessication upon drying or parting along laminae
- *Laminated Shale/Limestone* - typically has a slight to strong reaction to HCl due to the presence of limestone and thinly, <0.1ft, to thicker, >0.2ft laminations of shale and/or silt
- *Wackestone/Packstone* in Matrix- clasts of limestone in a fine grained matrix
- *Micrite* – a fine grained limestone showing a strong to violent reaction to HCl

Two of these lithologies are more accurately described as fine grained limestone (wackestone/packstone and micrite) that visually resembles shale yet is more cemented than actual shale. However, for the purpose of testing the sensitivity of the site ground motions to the presence of interbedded shale, each interval described as "shale" within the boring logs is considered to have the same shale characteristics described later in this section.

Vertical and Lateral Evaluation of Layer C Uniformity

An extensive review of 114 geotechnical core boring logs was performed to characterize the thickness, elevation and lithology of the "shale" intervals. As described above, irrespective of the actual detailed lithology, each "shale" layer was included in the following evaluation. Within Layer C there is a total of 112.5 feet of "shale" and 9455.9 total feet of limestone. The total percentage of "shale", calculated as the total thickness of "shale" divided by the total cored thickness of Layer C, is approximately 1.2 percent. With the exception of boring B-2002, which has a total of almost 11 cumulative feet of "shale" (all of which is more accurately either micrite or laminated limestone), the mean total shale thickness for all borings is less than 2 feet (1.2 percent) of Layer C.

The potential presence of laterally continuous shale layers was evaluated by plotting the thickness of shale within each boring at the respective elevation as shown on Figure A3-7. Also note on Figure A3-7 that the interface between the overlying Layer B2 and Layer C beneath Unit 4 indicates limited zones of shale in the range of elevation 782, which is the estimated mean average top elevation of Layer C. Subsection 2.5.4.12.4 of the FSAR provides a commitment that top of foundation inspections will identify shale pockets for removal prior to placement of fill or structural concrete, thus this horizon was not included in the following evaluation although the occurrence of shale was included in cumulative thickness and percentage estimates.

The main identified "shale" horizons include the following.

- Horizon CS1 ranges from about Elevation 766-763 and includes shale thicknesses from 0.2 to 1.5 ft thick.
- Horizon CS2 ranges from about Elevation 749-746 and includes shale thicknesses from 0.2 to 1.9 ft thick.
- Horizon CS3 ranges from about Elevation 745-742 and includes shale thicknesses from 0.2 to 2.6 ft thick.
- Horizon CS4 ranges from about Elevation 736-733 and includes shale thicknesses from 0.3 to 1.8 ft thick.

Each of these 4 shale horizons were plotted in plan view to determine their lateral extent, but they cannot be continuously mapped across the site. Regardless, these general characteristics of the site layers are used to develop representative model parameters for shale interbeds in Layer C.

Uniformity of Geophysical Measurements

Resistivity measurements were also used to evaluate the potential shale content within Layer C. The 15 borings with resistivity measurements were evaluated by using data from Layer D, a continuous shale layer beneath Layer C as a known baseline. Layer D has an average Single Point Resistance, (SPR) of approximately 12 to 16 Ohm. Within Layer C SPR varies from 28 to 80 Ohm, higher values than characteristic of shale at the site. SRP values at specific depths of known shale were also examined, and in general these values were also significantly higher than values characteristic of shale at the site. For example, at elevations 750.9 and 748.3 in Boring Log B-1000, a noted "shale" horizon, SPR values are 32-50 and 35-45 Ohm's respectively. These values that are higher than expected for shale are consistent with the detailed lithologic characteristics of the intervals that are more indicative of laminated shale/limestone. In summary, the resistivity measurements indicate that Layer C has relatively uniform characteristics that are more typical of limestone than shale.

Summary of Layer C Uniformity

A thorough evaluation of the core lithologic descriptions, photographs and geophysical measurements determined that shale is mostly limited to isolated pockets and not continuous layers within Layer C. Further, the total percentage of "shale" does not constitute a reduction in the mass properties of Layer C.

Layer C Base Case Parameters

Four base case models of alternate shale interbedding within Layer C were developed for this sensitivity analysis. These base cases were defined by: (1) the elevations and thicknesses of shale layers from the empirical data presented above, and (2) appropriate shear wave velocities of the shale layers and non-linear degredation properties for purposes of the sensitivity analyses.

Shale Interbed Base Case Models

The review of the core boring descriptions identified four specific characteristics of intervals described as "shale". Two of these are likely fine grained carbonate (micrite) as opposed to actual shale. However, for the purpose of this evaluation, each interval described as "shale" was classified in the sensitivity analysis with shale characteristics. The shale layers within Layer C for all borings are shown respective to elevation and noted thickness on Figure A3-7. Although planar maps clearly indicate that the shale cannot be mapped as laterally continuous layers, two alternate Base Case models of interval thickness and elevation were developed that effectively represent the shale interbeds as continuous layers (Figure A3-7).

Determination of Appropriate Shale Degradation Properties and Shear Wave Velocity

Development of representative shear modulus (G/Gmax) and damping ratio (D) versus shear strain relationships were developed through consultation with Dr. Ken Stokoe, Professor University of Texas. The G/G_{max} – log γ and D – log γ relationships for the various rock types at Comanche Peak are presented on Figures A2-1 and A2-2, respectively, in Appendix 2 of this report. As a point of comparison, Dr. Stokoe compared the relationships developed for the CPNPP and the dynamic laboratory test results that were conducted at the University of Texas in 2002 on shale core recovered from Oak Ridge, TN. Relationships for Oak Ridge shale in two conditions (weathered and unweathered) were used as bounding conditions. A more linear G/G_{max} – log γ and D – log γ relationships were noted to represent a lower bound for the unweathered shale (V_s in the lab ~ 4000 fps and V_s in the field ~ 5600 to 6200 fps). More nonlinear relationships were noted to represent weathered shale (V_s in lab ~ 3300 fps and V_s in the field ~ 5100 to 5500 fps). In both cases, the Oak Ridge cores were recovered from depths less than 200 ft.

Upon review, the lower bound relationships for the unweathered Oak Ridge shale are considerably more linear than the "shallow shale" G/G_{max} – log γ and D – log γ relationships presented for Comanche Peak. On the other hand, the weathered Oak Ridge shale relationships are considerably more non-linear than the Comanche Peak "shallow shale" relationships. Considering the unweathered nature and the somewhat lower field Vs values of the Comanche Peak shale, the relationships presented for Curve 4 in Figures A2-1 and A2-2 are considered appropriate for the Base Case models developed for the shale interbeds.

Based on these observations, a Vs of 3000 fps was used for one of the bounding Base Cases. A value significantly lower than measured velocities within Layer C and from weathered shale at Oak Ridge.

Base Case Models for Layer C

The following four cases were used as input to Sensitivity Run 3:

Case 1A: Layering from C Base 1 Model, Vs =5685, Curve 4 Figures A2-1, and A2-2
Case 1B: Layering from C Base 1 Model, Vs =3000, Curve 4 Figures A2-1, and A2-2
Case 2A: Layering from C Base 2 Model, Vs =5685, Curve 4 Figures A2-1, and A2-2
Case 2B: Layering from C Base 2 Model, Vs =3000, Curve 4 Figures A2-1, and A2-2

Sensitivity Run 3 Results

For these sensitivity calculations, the mean + 1 sigma total thickness of shale was used. Figures A3-8 through A3-11 show the calculated peak strains for all four cases considered. In the cases where the shale has a Vs of 5685 feet/sec (cases 1A and 2A), the strain on Layer C and the interbeds (depths of 40 to 105 ft) is fairly constant as a function of depth. In the cases where the shale has a Vs of 3000 feet/sec (cases 1B and 2B), the strain is significantly higher for the shale layers.

Figures A3-12 through A3-15 compare the summary statistics of the computed amplification factors from the four Run 3 cases to those used in FSAR Section 2.5 (identified as Original COLA). At frequencies above 1 Hz, the logarithmic-mean amplification factors are 10 to 25% lower for Run 3 cases than for Section 2.5. The standard deviations differ somewhat. In the cases where the shale has a Vs of 5685 feet/sec (cases 1A and 2A), the standard deviations are similar to Figure A3-3 and are due to the effects of full Vs correlation. In the cases where the shale has a Vs of 3000 feet/sec (cases 1B and 2B), the standard deviation is somewhat higher at frequencies near 20 Hz.

Considering that the shale Vs in cases 1A and 2A are the only ones that are consistent with the field Vs measurements, and that these two cases produce similar results to those in FSAR Section 2.5, it is concluded that the amplification factors in FSAR Section 2.5 are adequate.

Conclusions

The first sensitivity test shows small differences relative to the results in FSAR Section 2.5. The logarithmic-mean amplification factors are essentially identical. The differences in standard deviations are not large, and they do not show a definite pattern. Given the small extent of these differences, and the fact that the model of partial-correlation model for Vs is more credible than the full-correlation model, it is concluded that the amplification factors in FSAR Section 2.5 are adequate.

The second sensitivity test shows that the logarithmic-mean amplification factors obtained using nonlinear analysis are lower by 10 to 20% and the differences in standard deviations are associated with the assumption of full Vs correlation. It is concluded, therefore, that the amplification factors in FSAR Section 2.5 are adequate.

The third sensitivity test indicates that the logarithmic-mean amplification factors are 10 to 25% lower than in Section 2.5. The cases in which the interbedded shale has Vs values consistent with the field Vs measurements, the differences in standard deviations are somewhat different due to the effects of full Vs correlation. It is concluded, therefore, that the amplification factors in FSAR Section 2.5 are adequate.

In summary, the three sensitivity tests performed here indicate small differences with respect to the results contained in FSAR Section 2.5. Given the small extent of these differences, and the fact that the model parameters that lead to these differences are less tenable than the parameters used in FSAR Section 2.5, it is concluded that the results in FSAR Section 2.5 are adequate.

References

NEI White Paper, BNL Report N6112-051208, Rev. 1, "Consistent Site Response – SSI Calculations, June 12, 2009"

ISG-017, Interim Staff Guidance, on Ensuing Hazard Consistent Seismic Input for Site Response and Soil Structure Interaction Analyses, DC/COL.

Toro, G.R. (2005). Site-Wide Probabilistic Model of Shear-Wave Velocity Profiles at the Savannah River Site, Aiken, South Carolina. Report by Risk Engineering, Inc. to Bechtel Savannah River Co., October. Report Number WSRC-OS-2006-00514, Revision 1.

EPRI (Electric Power Research Institute) 1993. Appendices for Ground Motion Estimation. Volume 2 of Guidelines for Determining Design Basis Ground Motions. EPRI TR-102293. Palo Alto, California: Electric Power Research Institute.

Toro, G.R. (1996). Probabilistic Models Of Site Velocity Profiles For Generic And Site-Specific Ground-Motion Amplification Studies. Appendix C in Silva, W.J.; Abrahamson, N.; Toro, G.; and Costantino, C. (1996). Description and Validation of the Stochastic Ground Motion Model. El Cerrito, California: Pacific Engineering and Analysis.

Comanche Peak - Fully Correlated Profiles - Synthetic Profiles

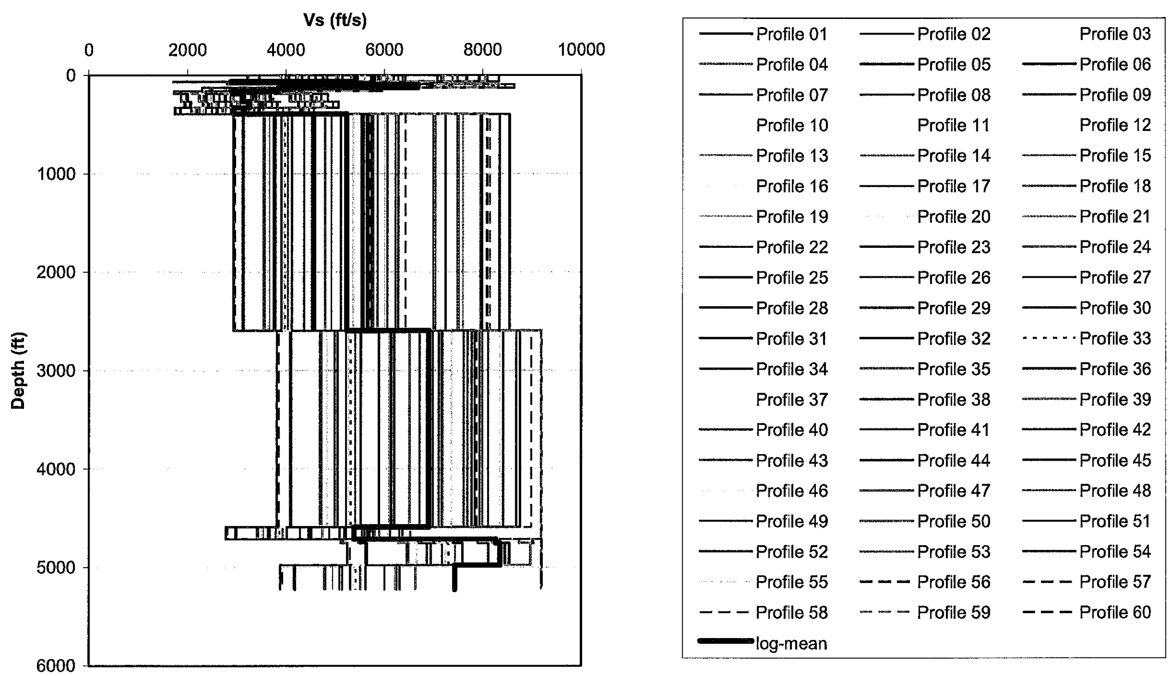

Figure A3-1. Randomized velocity profiles for Sensitivity Run 1 (entire soil column)

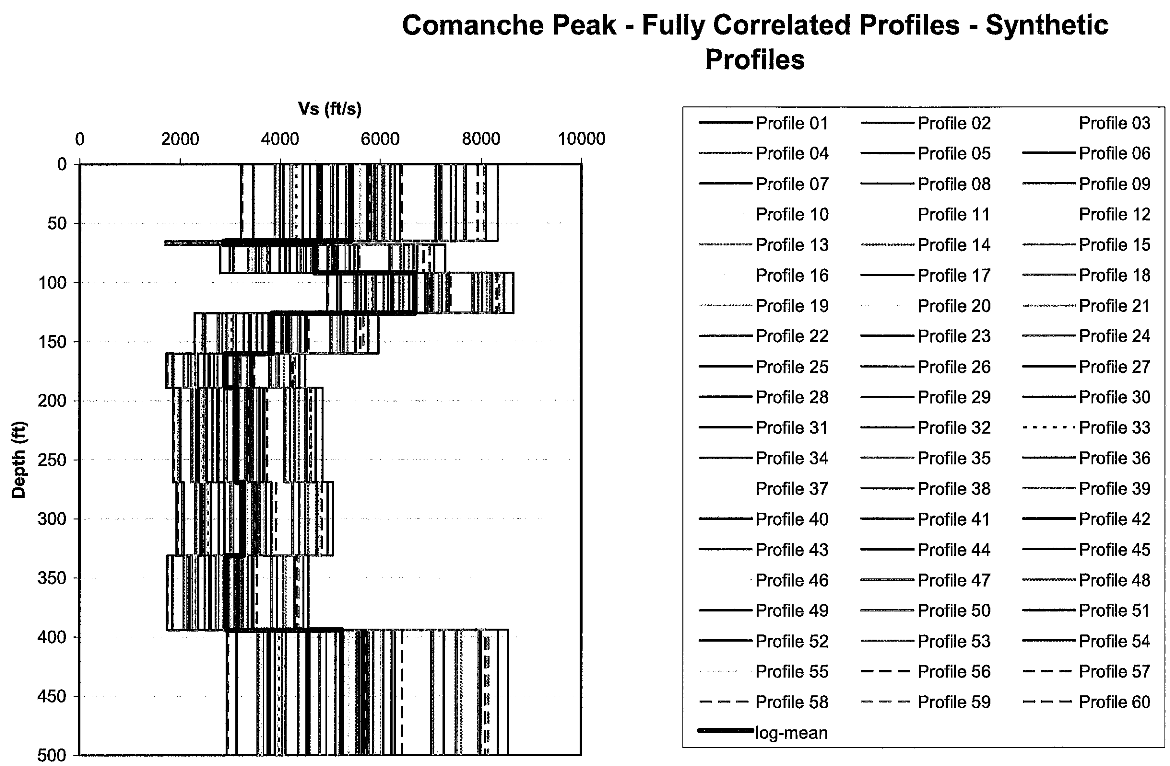

Figure A3-2. Randomized velocity profiles for Sensitivity Run 1 (top 500 feet)

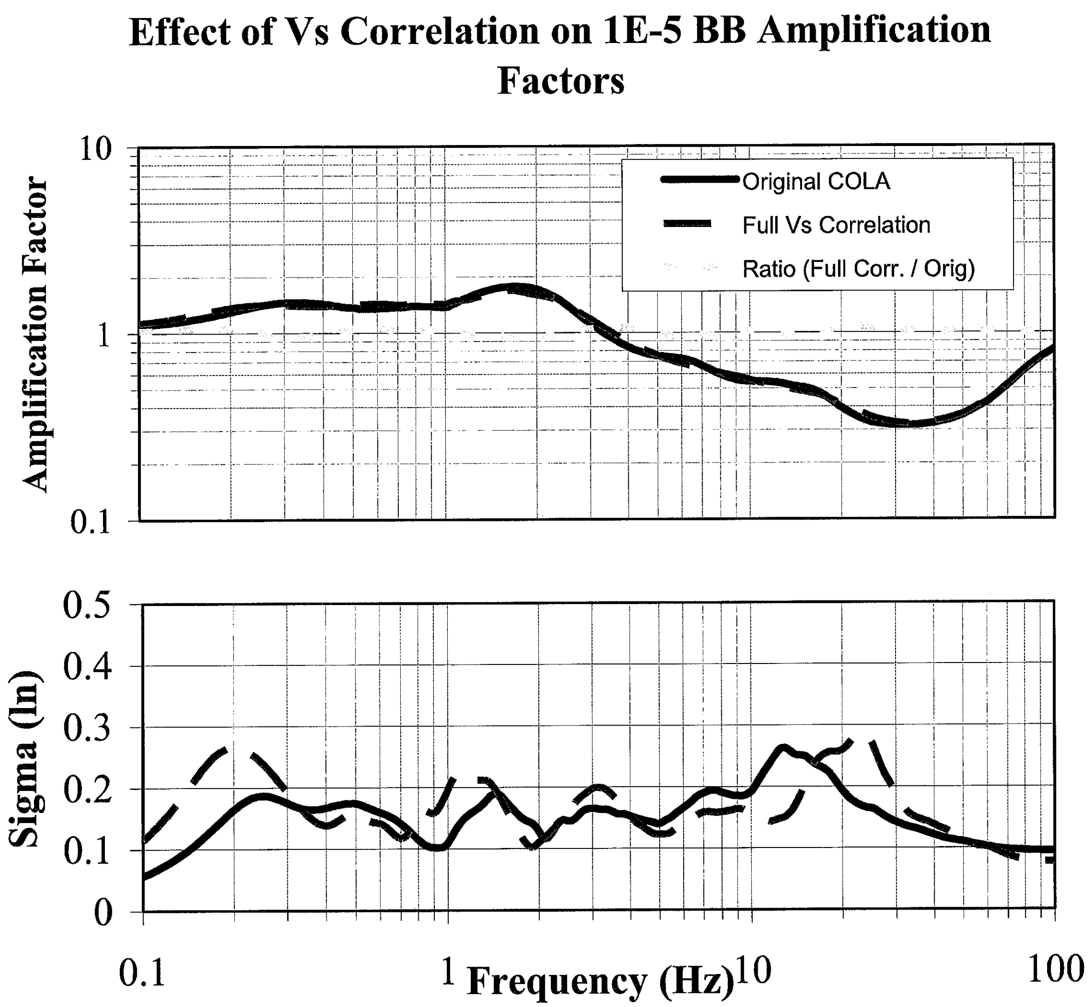

Figure A3-3. Comparison of amplification factors in Section 2.5 (original COLA) to those obtained using full Vs correlation. Top, logarithmic-mean amplification factors; bottom, logarithmic standard deviations.

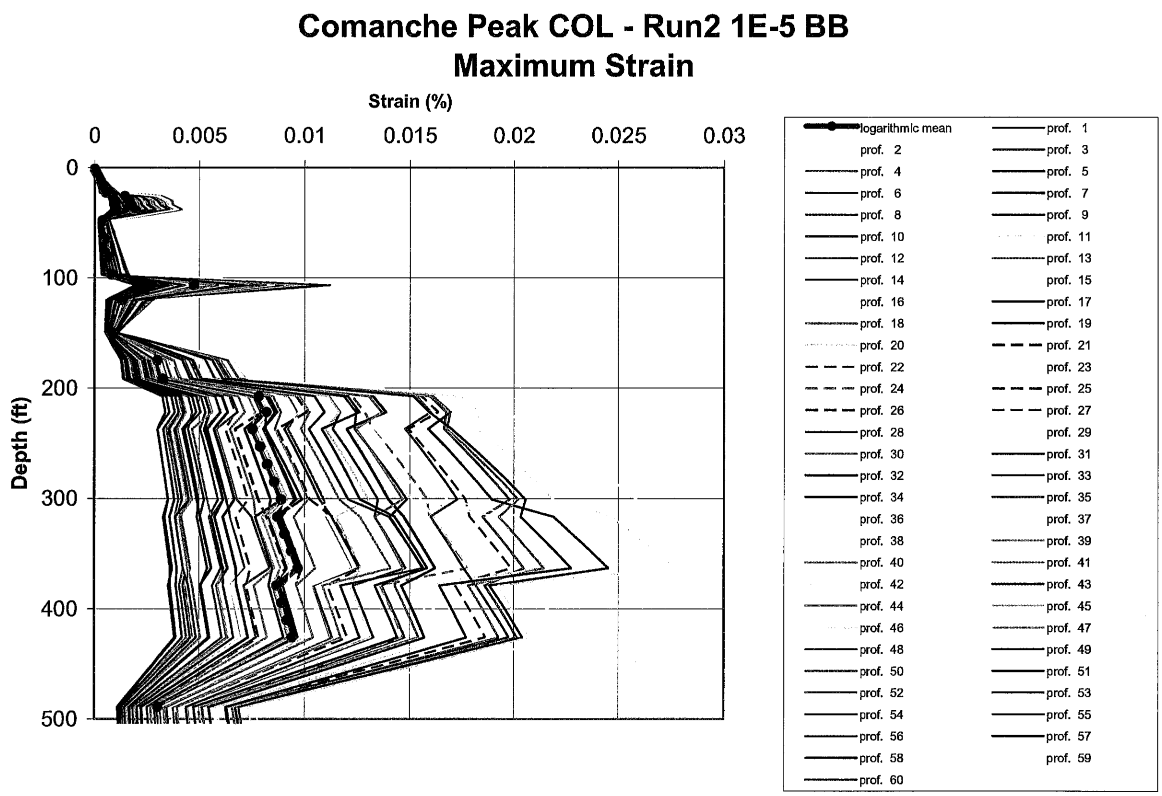

Figure A3-4. Peak strains for all 60 synthetic profiles considered in Run 2 (only the top 500 feet of the soil column are shown).

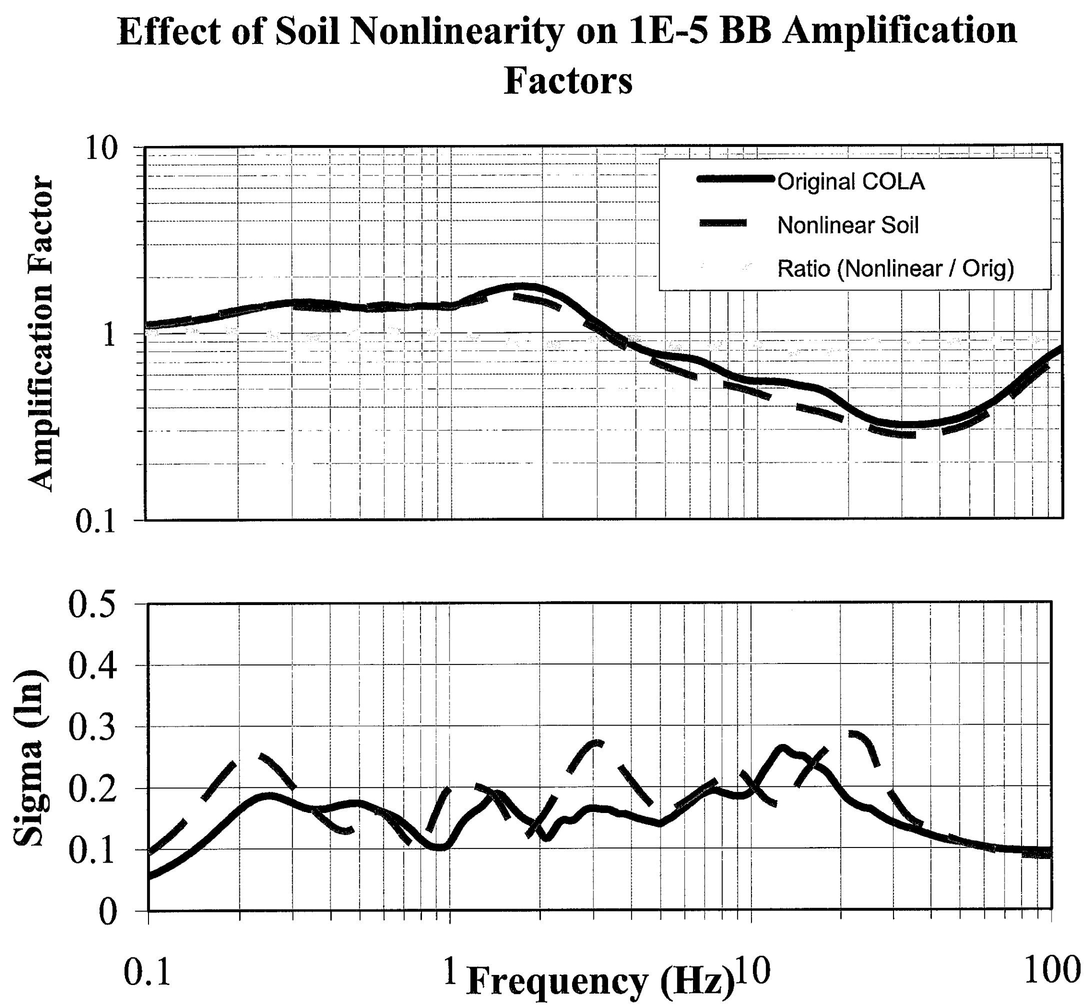

Figure A3-5. Comparison of amplification factors in Section 2.5 (original COLA) to those obtained using nonlinear soil properties and full Vs correlation (Run 2). Top, logarithmic-mean amplification factors; bottom, logarithmic standard deviations.

Effect of Soil Nonlinearity on 1E-5 BB Amplification Factors

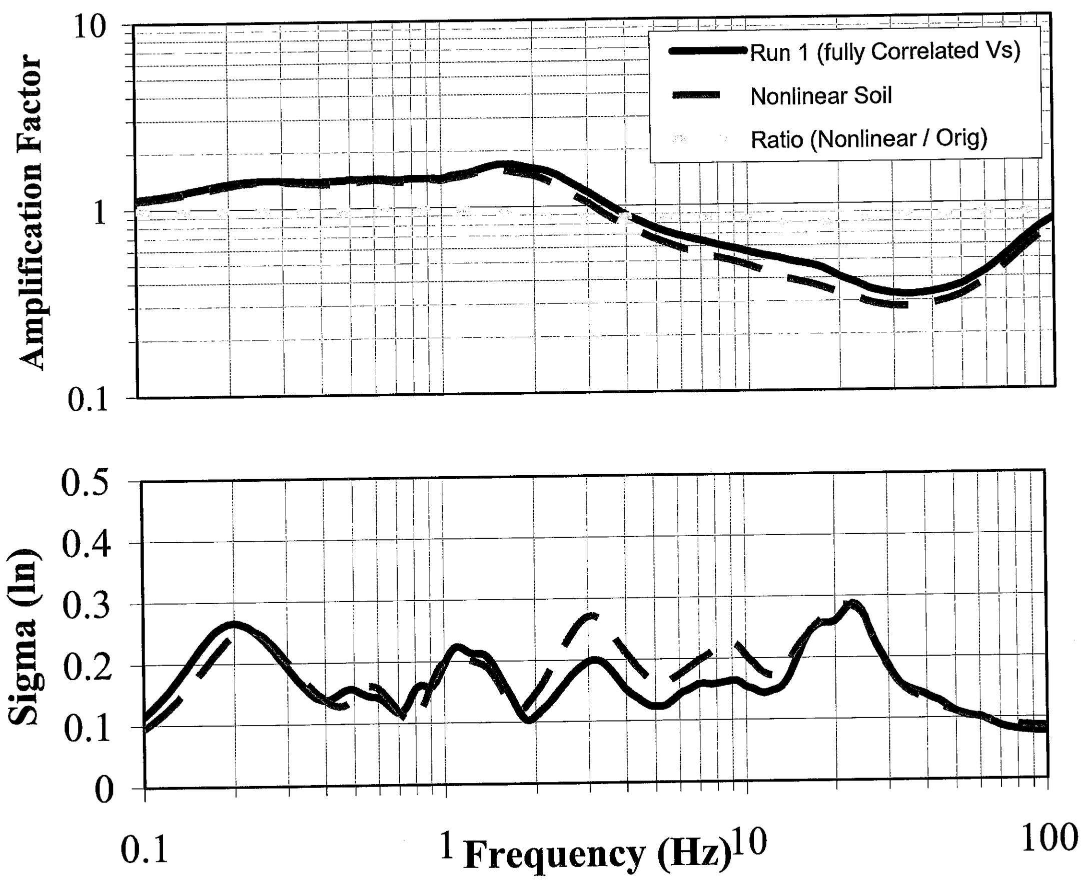

Figure A3-6. Comparison of amplification factors using linear soil properties and full Vs correlation (Run 1) to those obtained using nonlinear soil properties and full Vs correlation (Run 2). Top, logarithmic-mean amplification factors; bottom, logarithmic standard deviations.

FIGURE A3-7 was provided by WLA as a separate document (initially numbered A3-1)

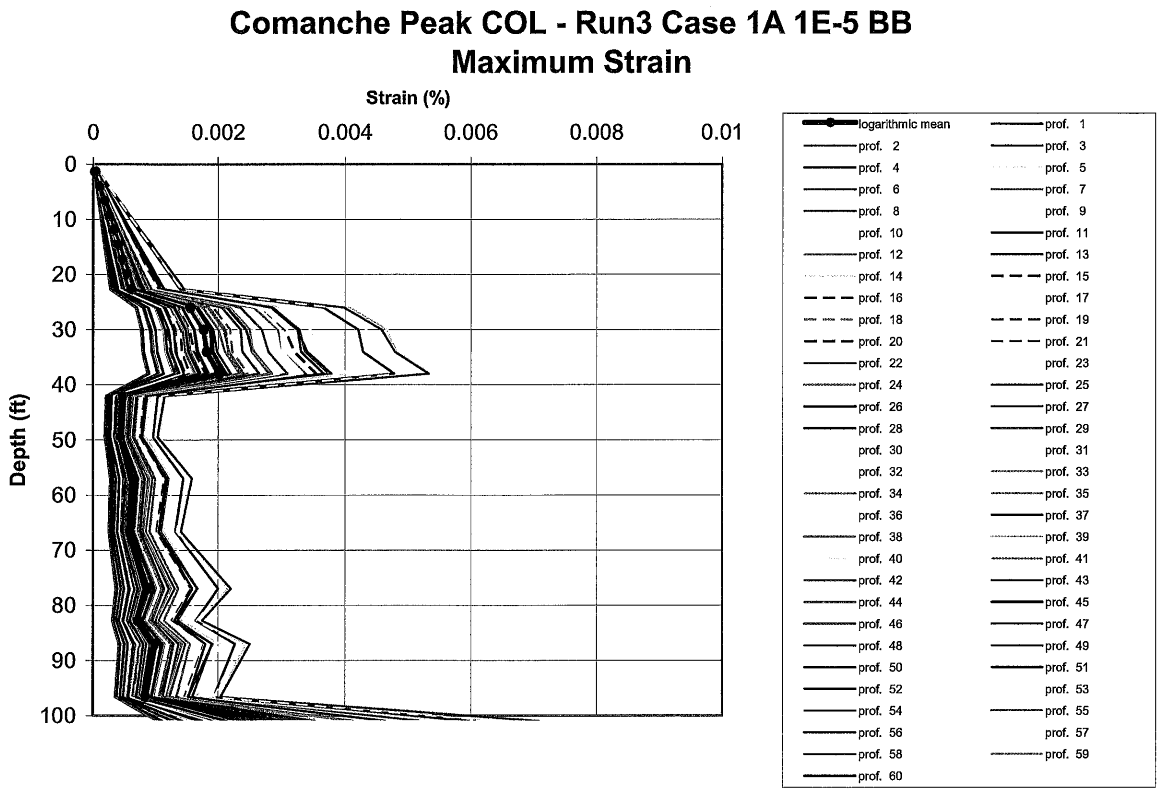

Figure A3-8. Peak strains for all 60 synthetic profiles considered in Run 3, Case 1a (only the top 100 feet of the soil column are shown).

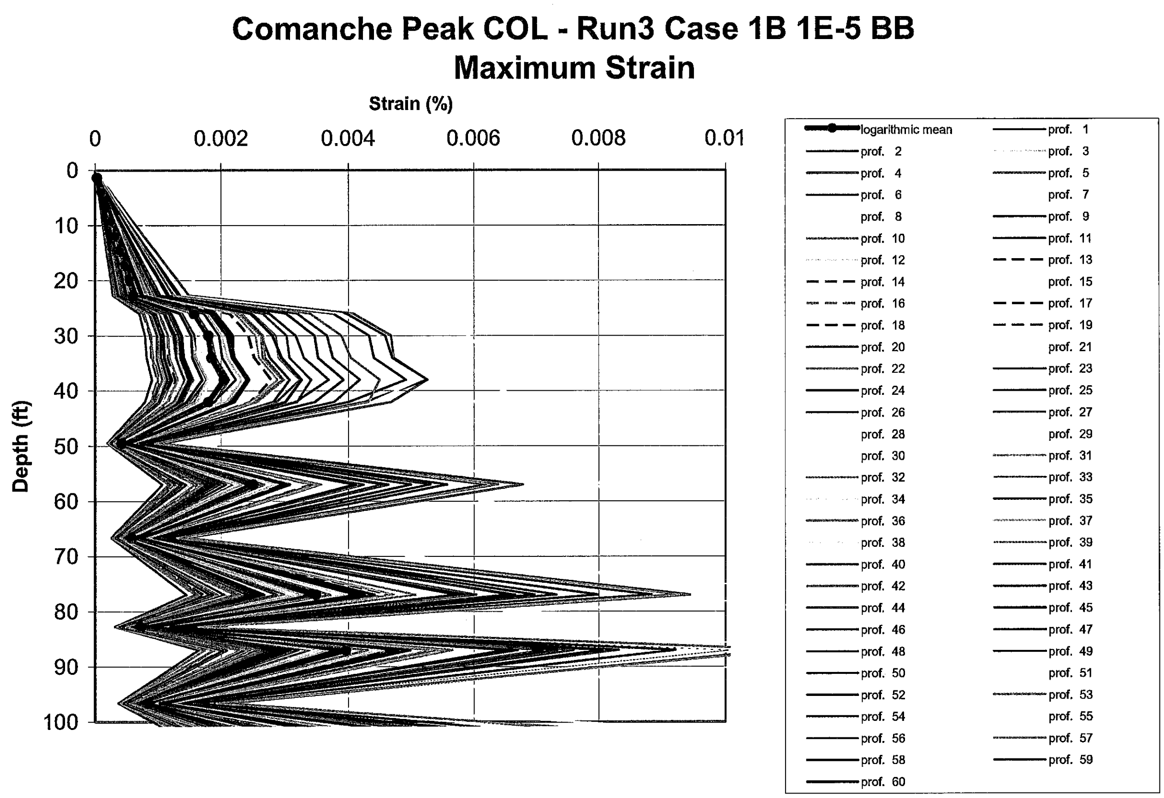

FigureA3-9. Peak strains for all 60 synthetic profiles considered in Run 3, Case 1b (only the top 100 feet of the soil column are shown).

Comanche Peak COL - Run3 Case 2a 1E-5 BB
Maximum Strain

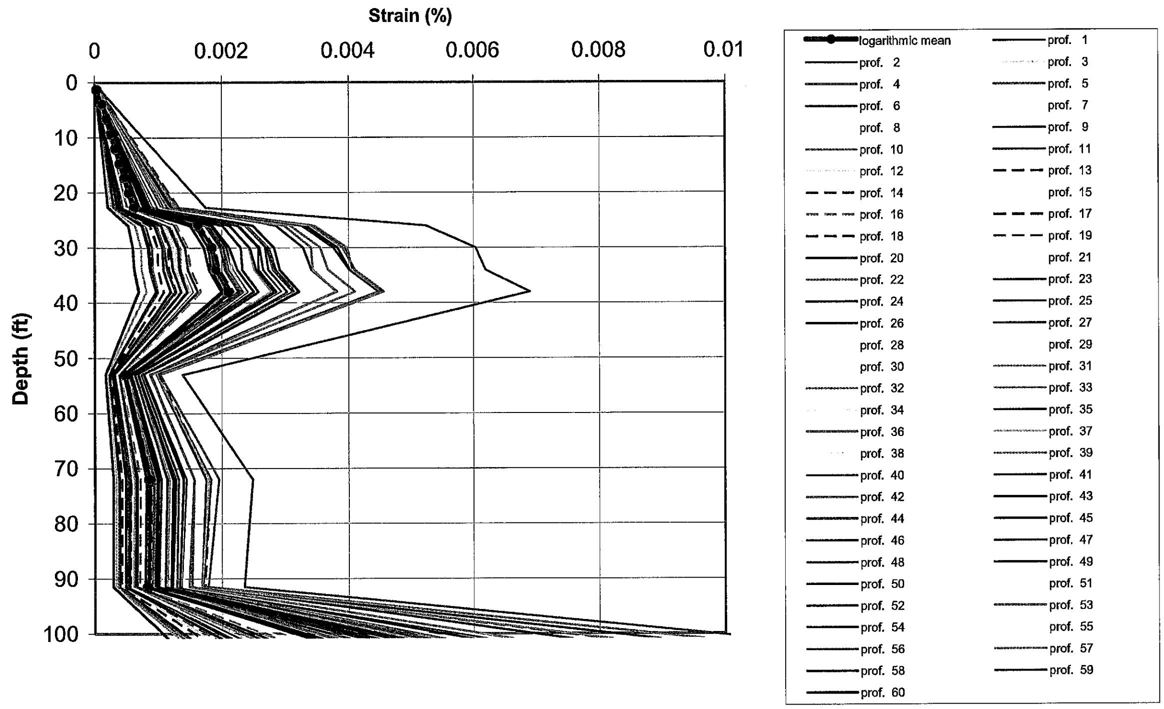

Figure A3-10. Peak strains for all 60 synthetic profiles considered in Run 3, Case 2a (only the top 100 feet of the soil column are shown).

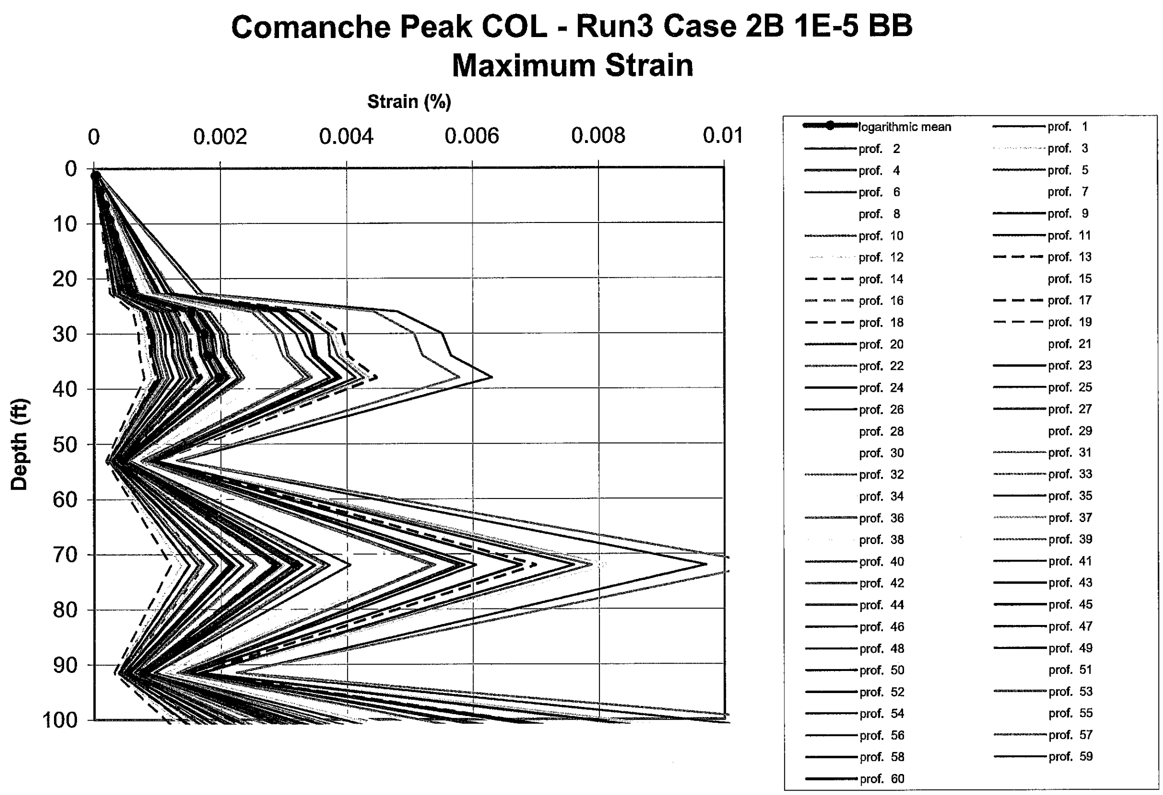

Figure A3-11. Peak strains for all 60 synthetic profiles considered in Run 3, Case 2b (only the top 100 feet of the soil column are shown).

Effect of Interbedded Shales (Case 1a) on 1E-5 BB Amplification Factors

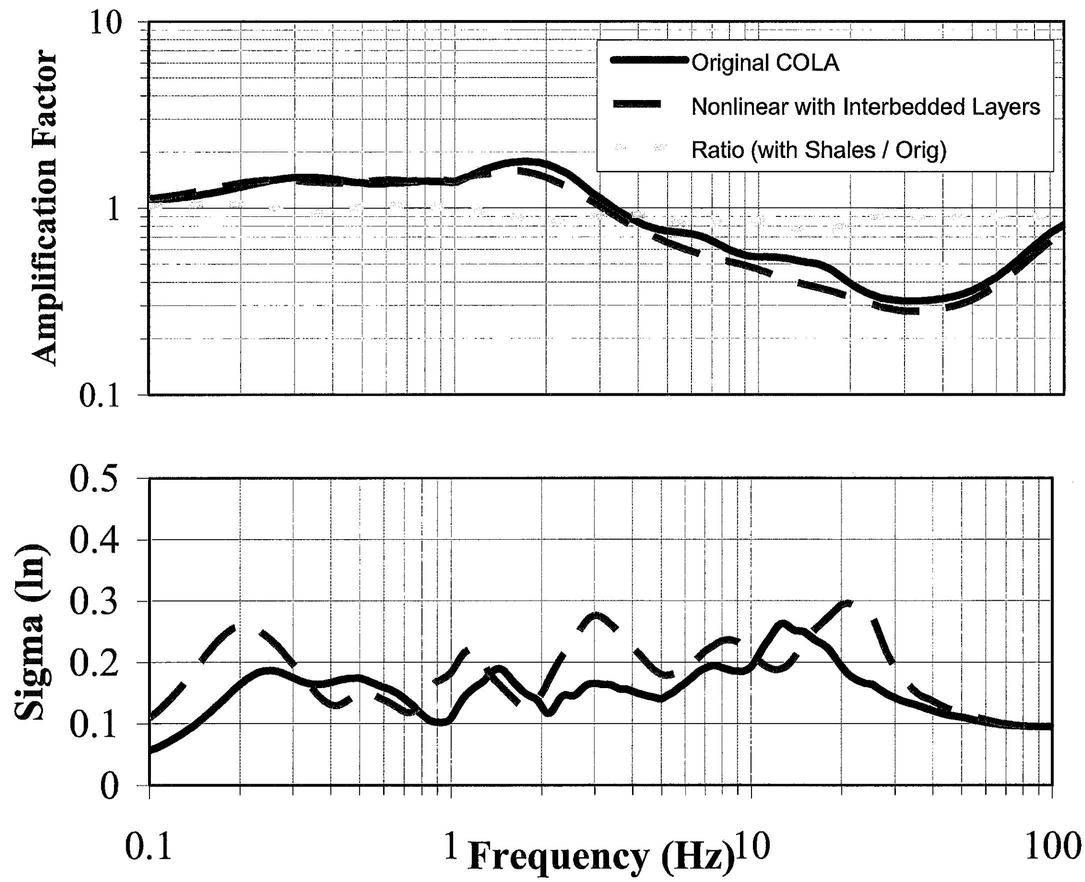

Figure A3-12. Comparison of amplification factors in Section 2.5 (original COLA) to those obtained using interbedded shale layers within Layer C (case 1a). Top, logarithmic-mean amplification factors; bottom, logarithmic standard deviations.

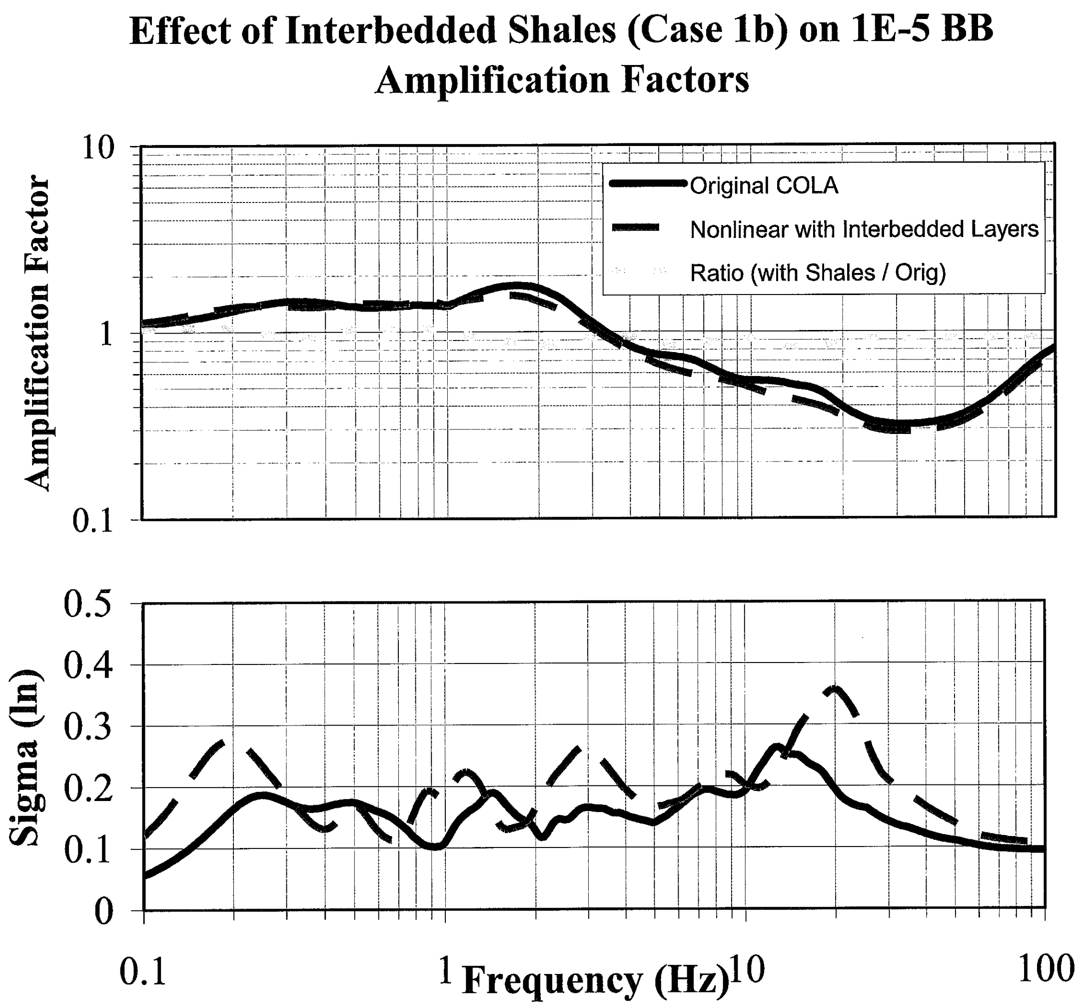

Figure A3-13. Comparison of amplification factors in Section 2.5 (original COLA) to those obtained using interbedded shale layers within Layer C (case 1b). Top, logarithmic-mean amplification factors; bottom, logarithmic standard deviations.

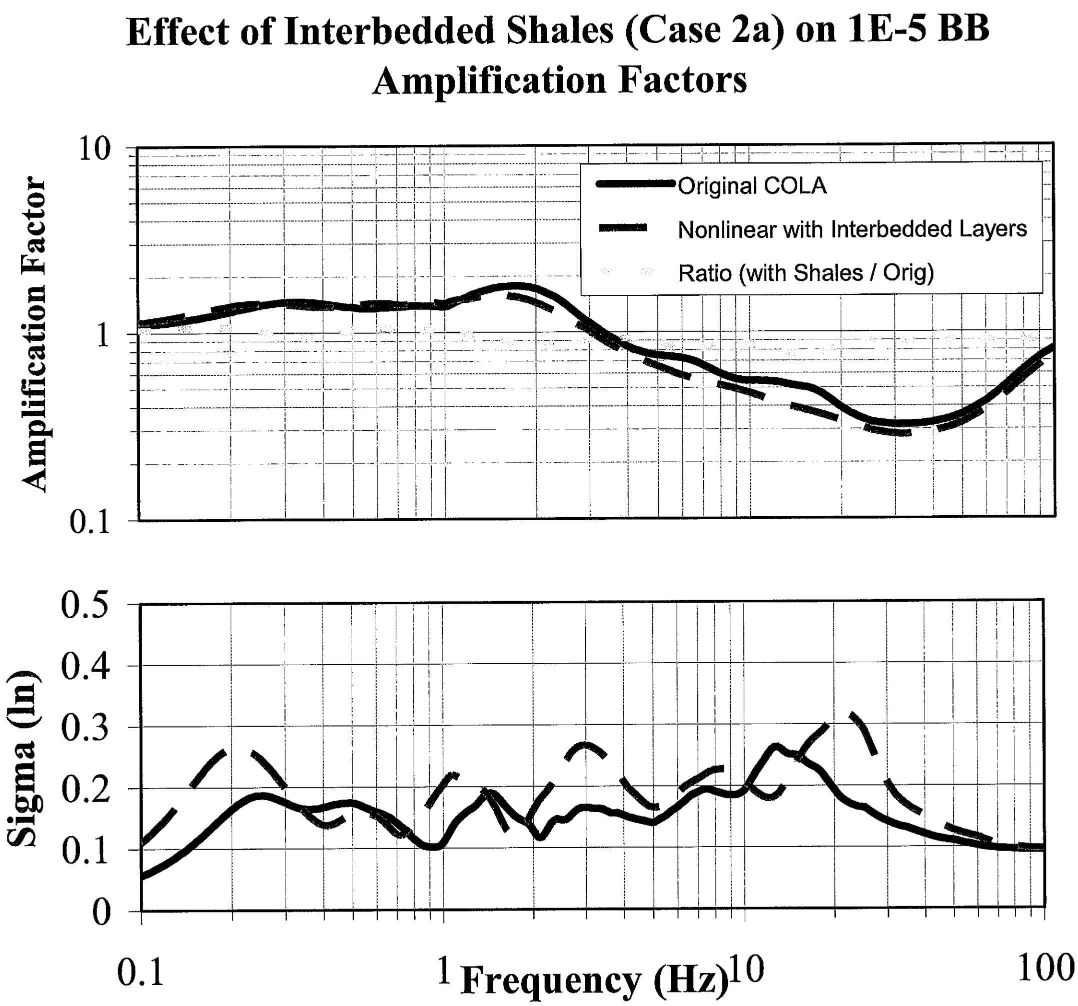

Figure A3-14. Comparison of amplification factors in Section 2.5 (original COLA) to those obtained using interbedded shale layers within Layer C (case 2a). Top, logarithmic-mean amplification factors; bottom, logarithmic standard deviations.

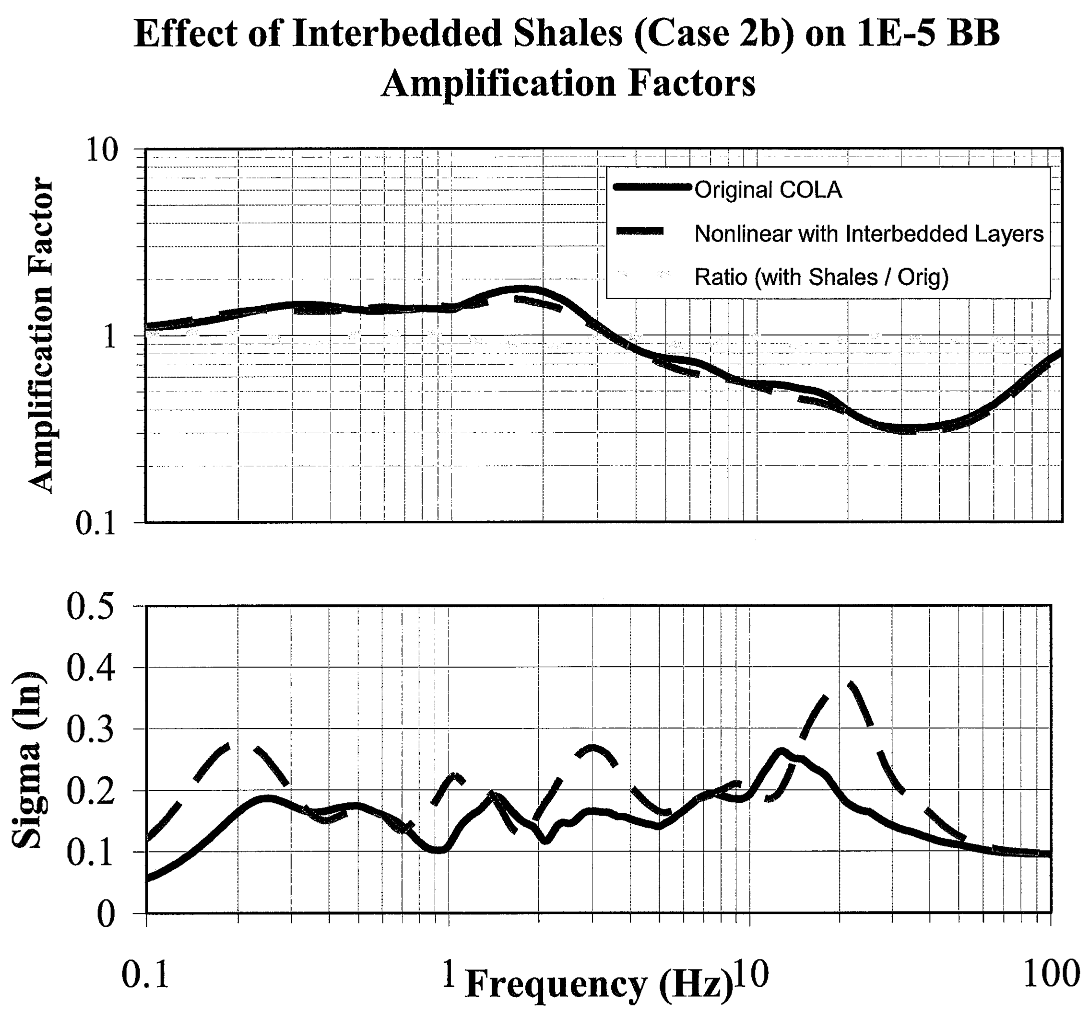

Figure A3-15. Comparison of amplification factors in Section 2.5 (original COLA) to those obtained using interbedded shale layers within Layer C (case 2b). Top, logarithmic-mean amplification factors; bottom, logarithmic standard deviations.